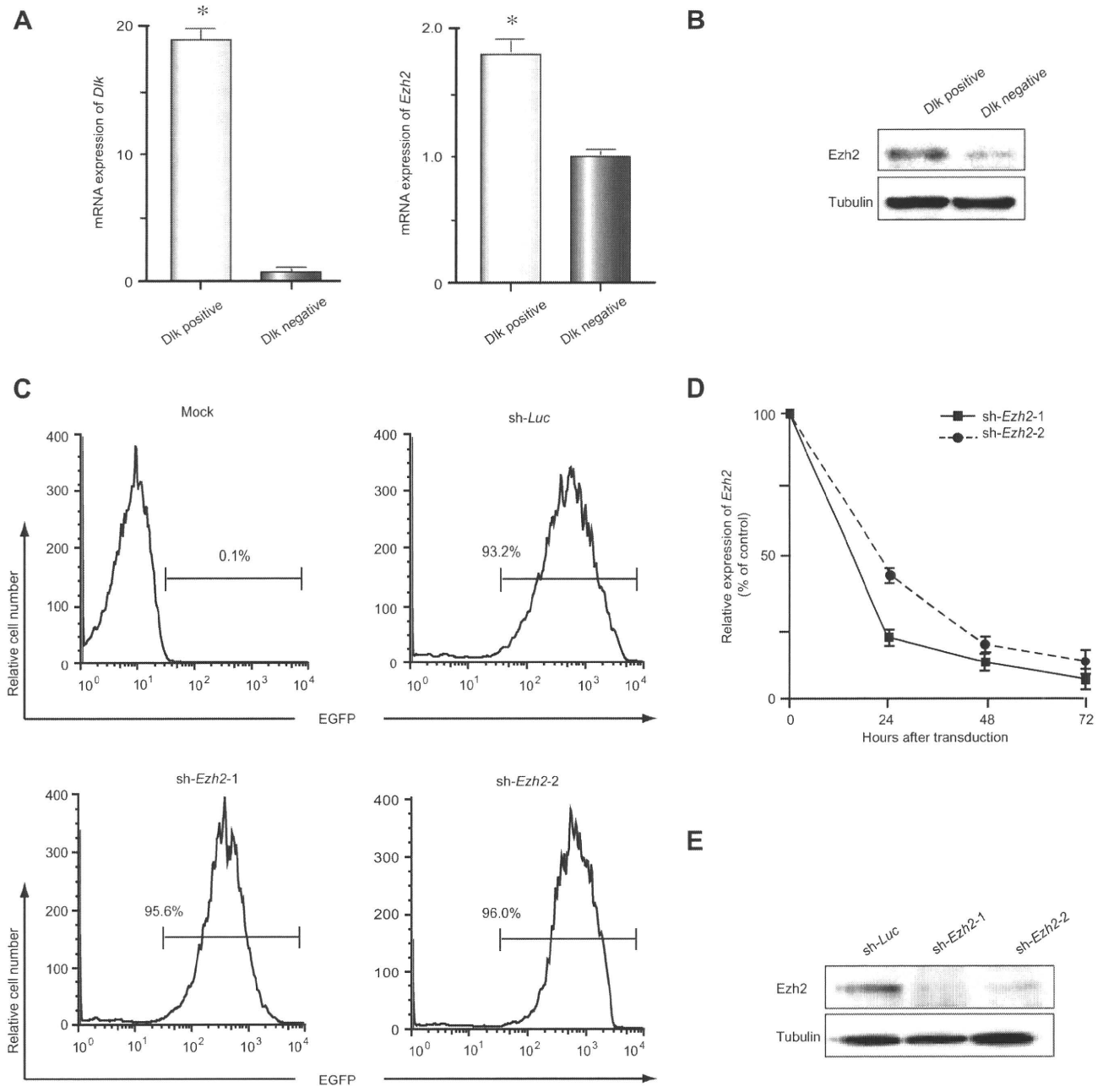

Fig. 1. Basal expression of *Ezh2* in wild-type and *Ezh2*-knockdown hepatic stem/progenitor cells. (A) Real-time RT-PCR analysis of *Dlk* and *Ezh2* expression in freshly purified Dlk$^+$ cells. *Statistically significant (p <0.05). (B) Western blot analysis of Ezh2 expression in freshly purified Dlk$^+$ cells compared to Dlk$^-$ cells. (C) The EGFP-positivity of cells transduced with indicated viruses. (D) Real-time RT-PCR analysis of *Ezh2* expression in Dlk$^+$ cells transduced with sh-*Ezh2*-1 or sh-*Ezh2*-2. A lentiviral vector expressing shRNA against *luciferase* (sh-*Luc*) was used as a control. Expression relative to the control is depicted. (E) Dlk$^+$ cells transduced with sh-*Ezh2*-1 or sh-*Ezh2*-2 were subjected to western blot analysis at day 5 of culture.

(Fig. 2C and D). Although *Ezh2*-knockdown enhanced apoptotic cell death in cultures of Dlk$^+$ cells, levels of apoptosis were not prominent in control or *Ezh2*-knockdown cultures (1.1 ± 0.2 and 3.6 ± 0.5%, respectively, Fig. 2E).

Among the colonies derived from hepatic stem/progenitor cells, those that keep growing beyond 28 days retain a significant number of hepatic stem/progenitor cells and efficiently generate secondary colonies in replating assays [6]. Because it is difficult to culture *Ezh2*-knockdown Dlk$^+$ cells beyond 14 days, we recovered cells from uninfected colonies that kept growing beyond 28 days and infected them with sh-*Ezh2* viruses. At day 7 of culture, Dlk$^+$EGFP$^+$ cells expressing sh-*Ezh2*-1 were collected by cell sorting and replated in order to allow the formation of colonies. The frequencies of total secondary colonies and large secondary colonies were markedly reduced by *Ezh2*-knockdown compared to the control (Fig. 2F). Again, the inhibitory effect of *Ezh2*-knock-

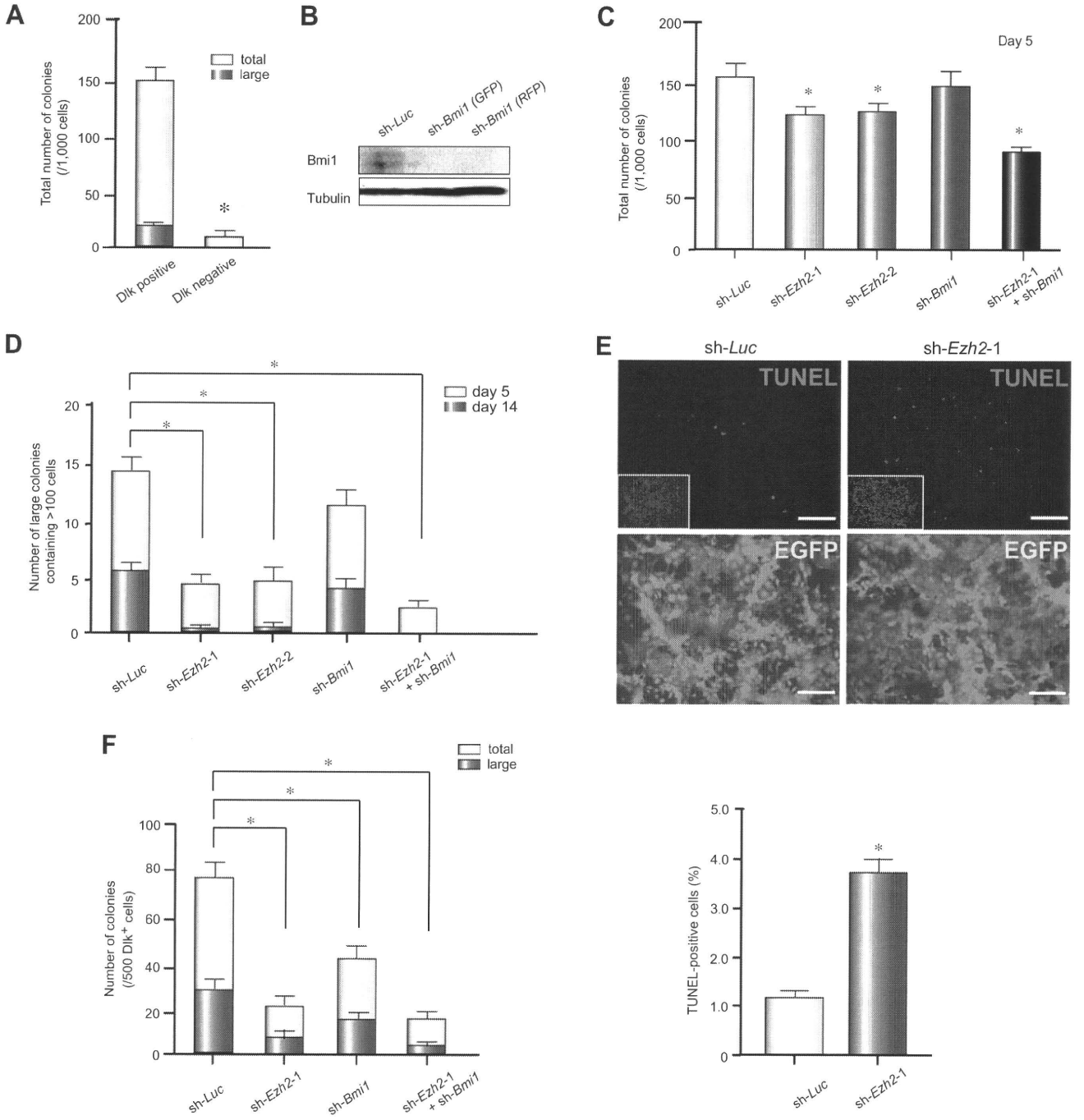

Fig. 2. Loss-of-function analyses of *Bmi1* and *Ezh2* on hepatic stem/progenitor cell proliferation. (A) The number of total colonies and large colonies consisting of more than 100 cells generated from 1000 Dlk$^+$ or Dlk$^-$ cells was counted at day 5 of culture. *Statistically significant (p <0.05) (B) Dlk$^+$ cells expressing shRNA against *Bmi1* together with *EGFP* or *RFP* as a marker gene were subjected to western blot analysis at day 5 of culture. (C) Numbers of colonies generated from 1000 Dlk$^+$ cells transduced with indicated viruses. Total numbers of colonies were counted at day 5 of culture. *Statistically significant (p <0.05) (D) The number of large colonies containing more than 100 cells at days 5 and 14. *Statistically significant (p <0.05). (E) TUNEL assays (upper panels) and fluorescence images (lower panels) of colonies at day 5 of culture. Nuclear DAPI staining (blue) is shown in the insets (upper panels). *Statistically significant (p <0.05). Scale bar = 500 μm. (F) Effect of *Ezh2*-knockdown on replating capacity. Among the colonies derived from uninfected Dlk$^+$ cells, those which kept growing beyond 28 days were infected with viruses expressing shRNAs. Seven days after infection, Dlk$^+$EGFP$^+$ cells were collected by cell sorting and replated to allow colonies to form. The total number of total colonies and large colonies consisting of more than 100 cells were counted at day 7 of subculture. *Statistically significant (p <0.05).

down was greater than that of *Bmi1*-knockdown, and double knockdown minimally enhanced the inhibitory effect of *Ezh2*-knockdown. These results suggest that Ezh2 plays an essential role in the maintenance of both the proliferative and self-renewal capacity in hepatic stem/progenitor cells. Colony PCR demonstrated that secondary large colonies expressed both hepatocyte

markers and cholangiocyte markers (Supplementary Fig. 1), indicating that the ability to differentiate into either hepatocytes or cholangiocytes was maintained in replated Dlk$^+$ cells. Of interest, the *Ezh2*-knockdown colonies showed a higher expression level of *albumin* (*Alb*) than the control colonies, whereas *Bmi1*-knockdown caused a mild increase in the expression of *Sall4*, which is a regulator of cholangiocyte differentiation [11].

Role of Ezh2 in differentiation of hepatic stem/progenitor cells

Ezh2 has recently been implicated in the differentiation of neural stem cells and epidermal stem cells [12,13]. However, its role in hepatic stem/progenitor cells remains to be addressed. In the control colonies, cytokeratin (CK) 7$^+$ cholangiocytes predominantly differentiated compared to Alb$^+$ hepatocytes. By contrast, comparable numbers of Alb$^+$ hepatocytes were detected in the colonies generated from *Ezh2*-knockdown Dlk$^+$ cells (Fig. 3A and B). Although *Bmi1*-knockdown did not significantly compromise the differentiation of Dlk$^+$ cells, double-knockdown colonies contained an increased number of Alb$^+$ hepatocytes as in *Ezh2*-knockdown (Fig. 3A and B). These results suggest that *Ezh2*-knockdown promotes the differentiation of hepatic stem/progenitor cells towards the hepatocyte lineage. Consistent with this finding, an enzyme-linked immunosorbent assay (ELISA) detected a significant increase in Alb secretion from culture of *Ezh2*-knockdown Dlk$^+$ cells compared to that of control Dlk$^+$ cells (Supplementary Fig. 2A). The expression of liver-enriched transcription factors was up-regulated in both *Ezh2*- and *Bmi1*-knockdown Dlk$^+$ cells at day 5 of culture (Fig. 3C). However, the increase was mild in the *Bmi1*-knockdown Dlk$^+$ cells compared to the *Ezh2*-knockdown or double-knockdown cells. A slight increase in the expression of *Sall4* was also observed in *Bmi1*-knockdown and double-knockdown cells. In clear contrast, neither *Ezh2*- nor *Bmi1*-knockdown Dlk$^+$ cells showed remarkable changes in the expression of *Gata1* (*GATA binding protein 1*), a haematopoietic transcription factor gene (Fig. 3C).

Regulation of the Ink4a/Arf gene by Ezh2

Bmi1, a core component of PRC1, regulates the self-renewal of various somatic stem cells, targeting $p16^{Ink4a}$ and $p19^{Arf}$ in particular [14,15]. Ezh2 likewise contributes to the repression of the *Ink4a/Arf* locus in mouse embryonic fibroblasts [16].

To examine whether *Ezh2*-knockdown results in derepression of the *Ink4a* and *Arf* genes, we performed real-time RT-PCR analyses. Expression of both $p16^{Ink4a}$ and $p19^{Arf}$ was up-regulated in *Ezh2*-knockdown Dlk$^+$ cells at day 5 of culture, although their derepression levels were moderate compared with those in *Bmi1*-knockdown cells (Fig. 4A). To address whether Ezh2 is involved in transcriptional repression through histone modifications at the *Ink4a/Arf* locus, we conducted ChIP analyses in wild-type Dlk$^+$ cells. ChIP assays demonstrated the binding of Ezh2 across the *Ink4a/Arf* locus and an increase in H3K27me3 levels (Fig. 4B).

Loss-of-function assays of Ezh2 in Ink4a/Arf$^{-/-}$ Dlk$^+$ cells

To evaluate directly the involvement of the *Ink4a/Arf* locus in Ezh2 function in hepatic stem/progenitor cells, we isolated Dlk$^+$ cells from *Ink4a–Arf*$^{-/-}$ embryos. Deletion of the *Ink4a/Arf* locus significantly enhanced the propagation of colonies compared to the wild-type Dlk$^+$ cells, and most of the colonies at day 5 of culture kept expanding up to day 14 (Fig. 5A and B). Flow-cytometric analysis at day 14 of culture revealed that the percentage of Dlk$^+$ cells in *Ink4a/Arf*$^{-/-}$ colonies was approximately 9-fold higher than in wild-type colonies (data not shown), indicating that deletion of the *Ink4a/Arf* locus enhanced the self-renewal capability of Dlk$^+$ cells. Notably, however, not only the total number of colonies but also the number of large colonies (consisting of more than 100 cells at day 5 of culture) was significantly reduced by *Ezh2*-knockdown (Fig. 5A and B). Consistent with this, the diameter of large *Ezh2*-knockdown colonies at day 14 of culture was significantly smaller than in the control (Fig. 5C). Of interest, the effect of *Bmi1*-knockdown was largely cancelled by the deletion of *Ink4a/Arf*, while that of *Ezh2*-knockdown was only partially abrogated (Fig. 5A–C). Immunostaining revealed that large colonies derived from *Ezh2*-knockdown *Ink4a-Arf*$^{-/-}$Dlk$^+$ cells still harboured a similar number of Alb$^+$ hepatocytes as those derived from *Ezh2*-knockdown wild-type Dlk$^+$ cells (Fig. 5D and E).

We next performed replating assays. At day 14 of culture, *Ink4a-Arf*$^{-/-}$Dlk$^+$EGFP$^+$ cells transduced with knockdown vectors were collected by cell sorting and replated to allow colonies to form. The frequency of total secondary colonies and of large secondary colonies was markedly reduced by *Ezh2*-knockdown compared to the control (Supplementary Fig. 3A). Deletion of the *Ink4a/Arf* locus cancelled out the effect of *Ezh2*-knockdown to a lesser extent than that of *Bmi1*-knockdown. Secondary colonies were generated in a similar fashion to the original colonies and exhibited enhanced differentiation towards the hepatocyte lineage (Supplementary Fig. 3B).

Role of Ezh2 in terminal differentiation and maturation in wild-type and Ink4a/Arf$^{-/-}$ Dlk$^+$ cells

We cultured Dlk$^+$ cells in EHS gel supplemented with OSM to selectively induce hepatocyte terminal maturation. By day 5 of culture, multiple cell clusters with tight cell–cell contact were formed. The *Ezh2*-knockdown clusters consisted of mature hepatocytes with a highly condensed, granulated cytosol and clear round nuclei compared with the control clusters (Fig. 6A). In addition, real-time RT-PCR revealed that tyrosine aminotransferase (*TAT*) and glucose-6-phosphatase (*G6P*), the metabolic enzyme genes highly expressed in terminally differentiated hepatocytes, were significantly up-regulated in *Ezh2*-knockdown cells (Fig. 6B). In addition, periodic acid-Schiff (PAS) staining successfully detected intracellular glycogen accumulation in *Ezh2*-knockdown cells, which indicated the functional maturation of the hepatocytes (Supplementary Fig. 2B). Although the deletion of *Ink4a/Arf* in Dlk$^+$ cells slightly promoted hepatocyte maturation in EHS gel cultures compared to wild-type Dlk$^+$ cells, *Ezh2*-knockdown further promoted hepatocyte maturation (Fig. 6A and B). Together, these findings indicate that post-commitment hepatocyte maturation is facilitated by *Ezh2*-knockdown.

Next, Dlk$^+$ cells were cultured on collagen type I gel in the presence of TNF-α to selectively induce differentiation into cholangiocytes. Both the control and *Ezh2*-knockdown cells similarly formed tube-like structures (Fig. 6C). Expression of *CK7*, *CK19* and integrin β4 (*Itgb4*), useful marker genes of cholangiocyte maturation, was mildly up-regulated in *Ezh2*-knockdown cells, but another marker gene, *Sall4*, did not show any changes in expression (Fig. 6D). The deletion of the *Ink4a/Arf* genes caused no

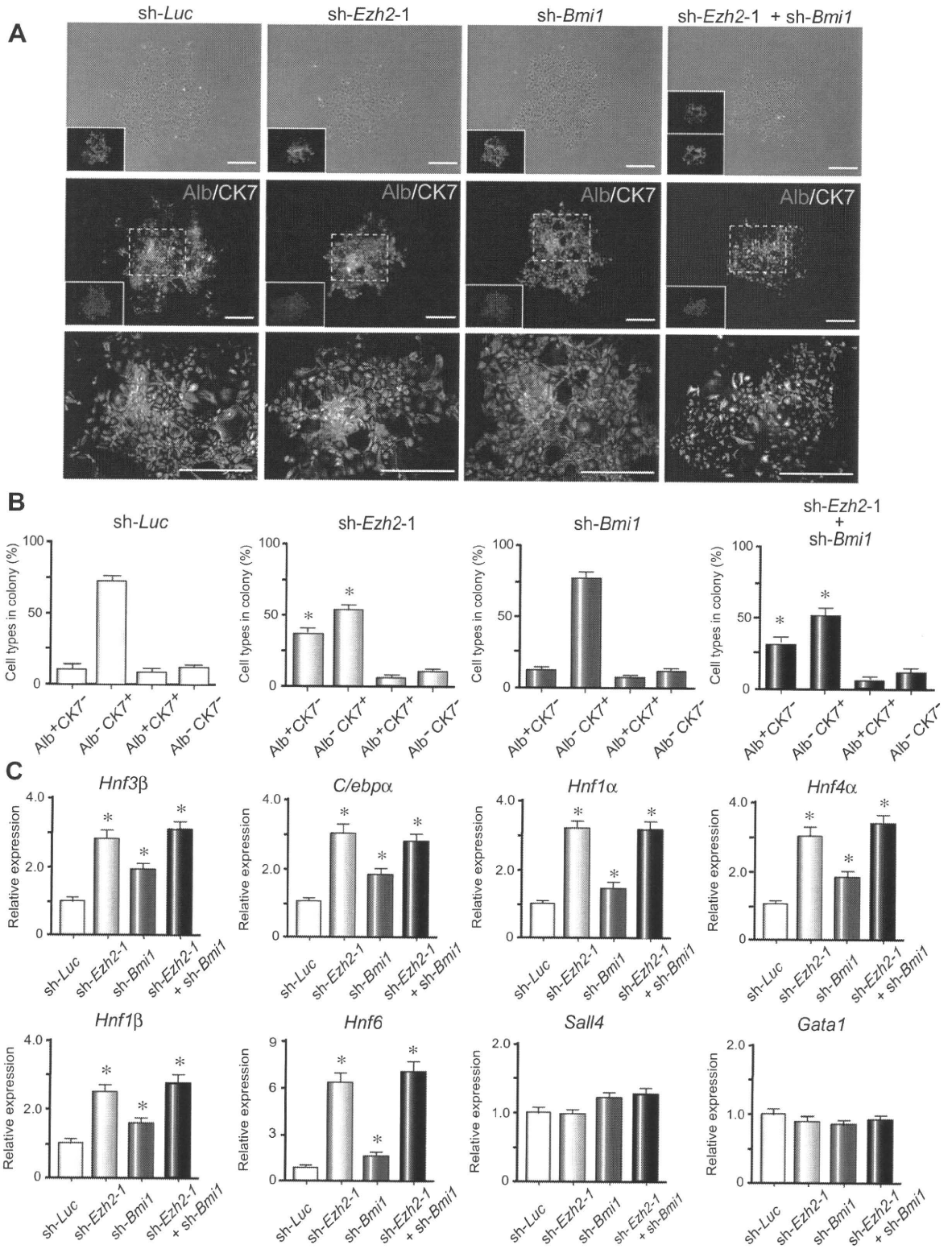

Fig. 3. Effects of *Ezh2*- and *Bmi1*-knockdown on the differentiation of hepatic stem/progenitor cells. (A) Bright-field images and fluorescence micrographs of large colonies (containing more than 100 cells) transduced with indicated viruses at day 5 of culture. Dual immunostaining was performed to detect the expression of Alb (red) and CK7 (green) in clonal colonies. EGFP expression in single-knockdown colonies, EGFP and RFP expression in a double-knockdown colony (upper panels) and nuclear DAPI staining (middle panels) are shown in the insets. Scale bar = 200 μm. (B) The percentages of Alb^+CK7^-, Alb^-CK7^+, Alb^+CK7^+, and Alb^-CK7^- cells in large colonies containing more than 100 cells were calculated at day 5 of culture. The average for 10 colonies is presented as the mean ± SD. *Statistically significant ($p < 0.05$). (C) Real-time RT-PCR analysis of the expression of liver-enriched transcription factors and *Gata1* in colonies derived from Dlk^+ cells transduced with indicated viruses at day 5 of culture. *Statistically significant ($p < 0.05$).

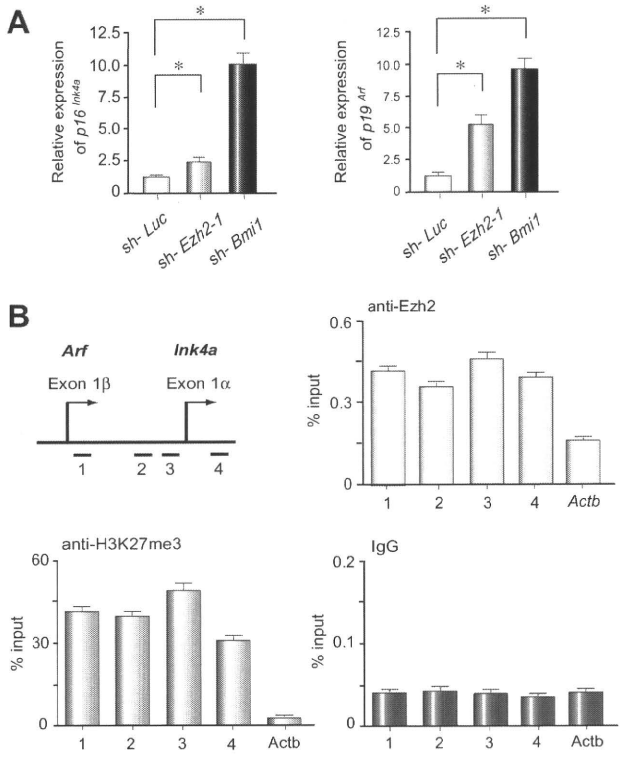

Fig. 4. Regulation of the *Ink4a/Arf* genes by Ezh2 in hepatic stem/progenitor cells. (A) Real-time RT-PCR analyses of $p16^{Ink4a}$ and $p19^{Arf}$ expression in colonies derived from Dlk$^+$ cells transduced with indicated viruses at day 5 of culture. *Statistically significant (p <0.05). (B) ChIP analyses of freshly purified Dlk$^+$ cells were conducted on the *Ink4a/Arf* locus (primer set 1–4) and the β-actin (*Actb*) control promoter region using indicated antibodies.

remarkable changes in collagen type I gel cultures in terms of cholangiocyte maturation (Fig. 6C and D).

Taken together, these findings indicate that post-commitment hepatocyte maturation rather than cholangiocyte maturation is accelerated by *Ezh2*-knockdown. Moreover, these results suggest that the *Ink4a/Arf* locus is also a major target of Ezh2, but there exist additional targets of Ezh2 in the regulation of hepatic stem/progenitor cell growth and self-renewal.

Discussion

Ezh2 plays an important role in gene silencing through the trimethylation of H3K27. In embryonic stem (ES) cells, most developmental genes are reversibly silenced through the bivalent domain in their transcriptional regulatory region, which consists of large regions of trimethylated H3K27 harbouring smaller regions of trimethylated H3K4 [17,18]. Therefore, PRC2 is critical in maintaining the pluripotency of embryonic stem (ES) cells. However, little is known about the role of PRC2 in somatic stem cells, especially in primary hepatic stem/progenitor cells. Our loss-of-function analysis of *Ezh2* clearly showed that Ezh2 regulates the proliferation of hepatic stem/progenitor cells in *Ink4a/Arf*-dependent and -independent manners. Given that *Ezh2*-knockdown profoundly affected the replating efficiency of hepatic stem/progenitor cells, Ezh2 might also be needed to maintain the self-renewal capacity of these cells. These functional characteristics of Ezh2 are very similar to those of Bmi1, but Ezh2 behaved quite differently from Bmi1 in the regulation of hepatic stem/progenitor cell differentiation. *Ezh2*-knockdown promoted the differentiation of hepatic stem/progenitor cells into hepatocytes and further enhanced the maturation of hepatocytes. However, *Bmi1*-knockdown did not compromise their differentiation. These findings unveil distinct functions of PRC1 and PRC2 in the regulation of hepatic stem/progenitor cell differentiation. A similar finding has been reported in breast cancer, in which EZH2 and BMI1 inversely correlate with prognosis and TP53 mutation [19].

Ink4a and *Arf* are major target genes of PcG proteins such as Bmi1 and Ezh2 [16]. Ezh2 contributes to the proliferation of pancreatic β-cells during regeneration by suppressing the *Ink4a/Arf* locus [20]. Overexpression of Ezh2 reportedly decreases expression of $p16^{INK4a}$ through hypermethylation of the $p16^{INK4a}$ promoter in cholangiocarcinogenesis in hepatolithiasis [21]. The present ChIP analyses showed that Ezh2 binds to the *Ink4a/Arf* locus, accompanied by increased levels of trimethylated H3K27 in hepatic stem/progenitor cells. However, deletion of the *Ink4a/Arf* locus only partially abrogated the inhibitory effect of *Ezh2*-knockdown on the expansion of hepatic stem/progenitor cells. On the other hand, the inhibitory effect of *Bmi1*-knockdown was largely cancelled by deletion of *Ink4a/Arf*. These results indicate that Ezh2 regulates hepatic stem/progenitor cells in both *Ink4a/Arf*-dependent and -independent manners. Actually, double knockdown of *Ezh2* and *Bmi1* had a limited advantage over single knockdown of *Ezh2* in inhibiting hepatic stem/progenitor cell proliferation, further indicating additional functions of Ezh2 independent of Ink4a/Arf.

A number of liver-enriched transcription factors, including hepatocyte nuclear factors (Hnfs) and CCAAT/enhancer binding proteins (Cebps), play a central role in normal hepatogenesis [22]. It has been reported that Hnf3β, a marker of definitive endoderm, is indispensable for early liver development [23]. Consistent with this, enforced expression of Hnf3β in ES cells and mesenchymal stem cells promotes differentiation towards the hepatocyte lineage [24,25]. Recent studies have shown that Cebpα, a nuclear transcription factor of the bZIP protein family, is essential for hepatocyte differentiation [26]. In addition, suppression of Cebpα expression stimulates biliary cell differentiation, with reduced expression of Hnf6 and Hnf1β [27].

In the present study, *Ezh2*-knockdown in hepatic stem/progenitor cells resulted in enhanced expression of Hnfs. Likewise, increased expression of *Hnf6* and *Hnf1b* was simultaneously observed. Of interest, chromatin immunoprecipitation combined with DNA microarray (ChIP-on-chip) analyses reveal that both PRC1 and PRC2 can bind to the promoter regions of *Hnf3b*, *Cebpa*, and *Hnf6* in ES cells [28]. As *Hnf3b* and *Cebpa* have bivalent domains in their promoter regions [17,18], we hypothesised that *Ezh2* mediates the silencing of these genes to maintain hepatic stem/progenitor cells in an immature state. Unexpectedly, the present ChIP analyses using purified Dlk$^+$ cells failed to demonstrate the binding of Ezh2 at these loci (data not shown). It is possible that the Dlk$^+$ fraction was inappropriate for detecting the recruitment of Ezh2 for repression of target genes because it contained not only stem/progenitor cells but also cells in different stages of differentiation. Intriguingly, a recent study showed that Ezh2-dependent trimethylated H3K27 prevents the recruitment of AP1 and other transcription factors required for terminal differentiation [13]. It is also possible that Ezh2-dependent H3K27me3 on hepatocyte differentiation-related genes likewise

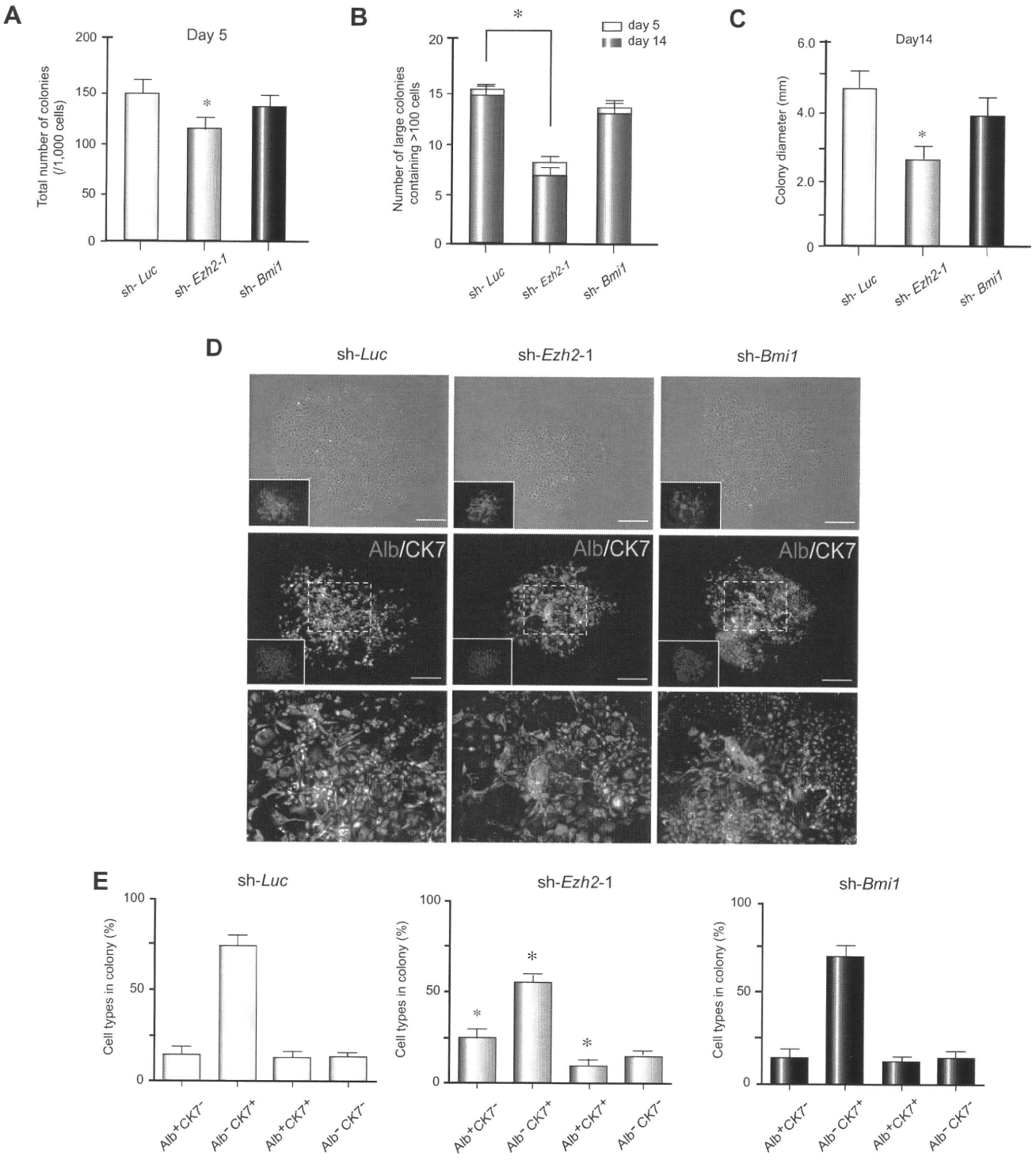

Fig. 5. Loss-of-function analyses of *Bmi1* and *Ezh2* on the proliferation of *Ink4a–Arf*$^{-/-}$ hepatic stem/progenitor cells. (A) Numbers of colonies generated from 1000 *Ink4a–Arf*$^{-/-}$Dlk^{+} cells transduced with indicated viruses. Total numbers of colonies were counted at day 5 of culture. *Statistically significant (p <0.05) (B) The number of large colonies containing more than 100 cells at days 5 and 14. *Statistically significant (p <0.05). (C) The diameter of large colonies at day 14 of culture. *Statistically significant (p <0.05). (D) Bright-field images and fluorescence micrographs of large colonies (containing more than 100 cells) transduced with indicated viruses at day 5 of culture. Dual immunostaining was performed to detect the expression of Alb (red) and CK7 (green) in clonal colonies. EGFP expression (upper panels) and nuclear DAPI staining (middle panels) are shown in the insets. Scale bar = 200 μm. (E) The percentages of Alb^{+}CK7^{-}, Alb^{-}CK7^{+}, Alb^{+}CK7^{+}, and Alb^{-}CK7^{-} cells in large colonies containing more than 100 cells were calculated at day 5 of culture. The average for 10 colonies is presented as the mean ± SD. *Statistically significant (p <0.05).

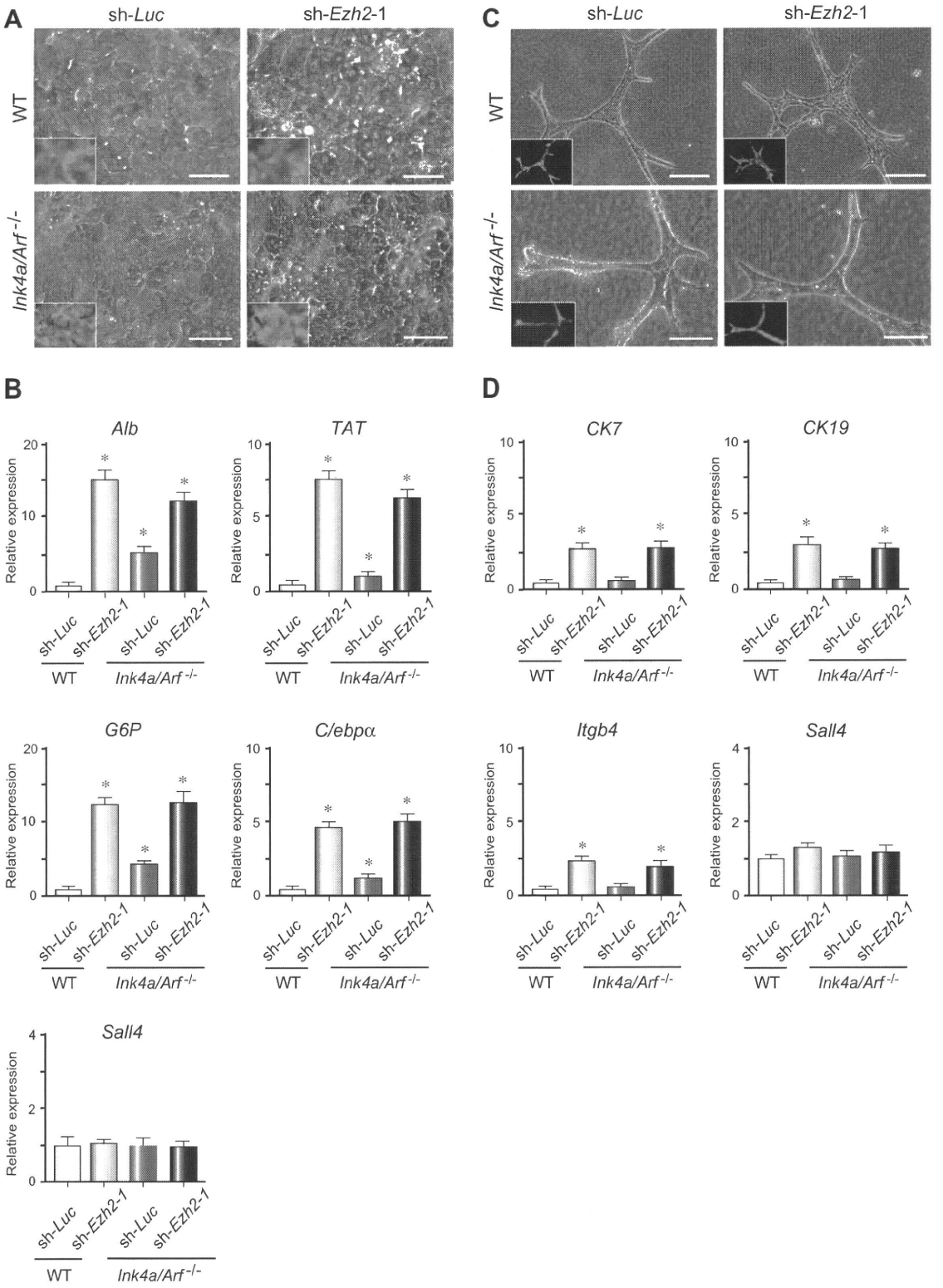

Fig. 6. Terminal differentiation of *Ezh2*-knockdown Dlk$^+$ cells towards hepatocytes and cholangiocytes. (A) To evaluate the terminal differentiation of wild-type or *Ink4a–Arf*$^{-/-}$Dlk$^+$ cells towards hepatocytes, *Ezh2*-knockdown Dlk$^+$ cells were placed on EHS gel in the presence of OSM. Bright-field images and fluorescence micrographs (inset panels) of cells in EHS gel at day 5 of culture are presented. Scale bar = 100 μm. (B) Real-time RT-PCR analyses of hepatocyte differentiation and maturation marker genes. *Statistically significant (p <0.05). (C) To evaluate the terminal differentiation of wild-type or *Ink4a–Arf*$^{-/-}$Dlk$^+$ cells towards cholangiocytes, *Ezh2*-knockdown Dlk$^+$ cells were subjected to collagen gel culture in the presence of TNF-α. Bright-field images and fluorescence micrographs (inset panels) of cells in collagen type I gel at day 5 of culture are presented. Scale bar = 100 μm. (D) Real-time RT-PCR analyses of cholangiocyte differentiation and maturation marker genes. *Statistically significant (p <0.05).

prevents the recruitment of liver-enriched transcription factors in hepatic stem/progenitor cells.

Although PcG proteins have been characterised as self-renewal factors of embryonic as well as somatic stem cells, Ezh2 has recently been implicated in the differentiation of neural stem cells and epidermal stem cells [12,13]. Our findings further support an essential role for PcG proteins in the precise regulation of stem cell differentiation. The composition of PcG complexes is highly dynamic and differs among different cell types and even at different gene loci. Given that the complexes exhibit differences in specificity for histone substrates, the target genes regulated by PcG proteins are quite diverse among different cell types [29]. Efforts to unravel the molecular machinery of PcG proteins, including Ezh2, would facilitate our overall understanding of the hepatic stem cell system and contribute to the establishment of liver regeneration therapy.

Conflicts of interest

The Authors who have taken part in this study declared that they do not have anything to disclose regarding funding or conflict of interest with respect to this manuscript.

Acknowledgements

The authors thank Dr. Kristian Helin for the anti-Ezh2 antibody, Dr. Hiroyuki Miyoshi for the CS-H1-shRNA-EF-1α-EGFP and CS-H1-shRNA-RfA-ERP vectors, Dr. Akihide Kamiya for technical assistance and Mieko Tanemura for laboratory assistance.
Financial support: This work was supported in part by grants for the Global COE program (Global Center for Education and Research in Immune System Regulation and Treatment) from the Ministry of Education, Culture, Sports, Science and Technology, Japan, and grants from the Core Research for Evolutional Science and Technology (CREST) of Japan Science and Technology Corporation (JST), the Takeda Science Foundation, and the Uehara Memorial Foundation.

Appendix A. Supplementary data

Supplementary data associated with this article can be found, in the online version, at doi:10.1016/j.jhep.2010.01.027.

References

[1] Fausto N. Liver regeneration and repair: hepatocytes, progenitor cells, and stem cells. Hepatology 2004;39:1477–1487.
[2] Tanimizu N, Nishikawa M, Saito H, Tsujimura T, Miyajima A. Isolation of hepatoblasts based on the expression of Dlk/Pref-1. J Cell Sci 2003;116:1775–1786.
[3] Tanimizu N, Hiroki S, Keith M, Miyajima A. Long-term culture of hepatic progenitors derived from mouse Dlk$^+$ hepatoblasts. J Cell Sci 2004;117:6425–6434.
[4] Pietersen AM, van Lohuizen M. Stem cell regulation by polycomb repressors: postponing commitment. Curr Opin Cell Biol 2008;20:201–207.
[5] Yonemitsu Y, Imazeki F, Chiba T, Fukai K, Nagai Y, Miyagi S, et al. Distinct expression of polycomb group proteins EZH2 and BMI1 in hepatocellular carcinoma. Hum Pathol 2009;40:1304–1311.
[6] Chiba T, Zheng YW, Kita K, Yokosuka O, Saisho H, Onodera M, et al. Enhanced self-renewal capability in hepatic stem/progenitor cells drives cancer initiation. Gastroenterology 2007;133:937–950.
[7] Kamiya A, Kinoshita T, Ito Y, Matsui T, Morikawa Y, Senba E, et al. Fetal liver development requires a paracrine, action of oncostatin M through the gp 130 signal transducer. EMBO J 1999;18:2127–2136.
[8] Nishikawa Y, Tokusashi Y, Kadohama T, Nishimori H, Ogawa K. Hepatocytic cells form bile duct-like structures within a three-dimensional collagen gel matrix. Exp Cell Res 1996;223:357–371.
[9] Negishi M, Saraya A, Miyagi S, Nagao K, Inagaki Y, Nishikawa M, et al. Bmi1 cooperates with Dnmt1-associated protein 1 in gene silencing. Biochem Biophys Res Commun 2007;353:992–998.
[10] Tzatsos A, Pfau R, Kampranis SC, Tsichlis PN. Ndy1/KDM2B immortalizes mouse embryonic fibroblasts by repressing the Ink4a/Arf locus. Proc Natl Acad Sci USA 2009;106:2641–2646.
[11] Oikawa T, Kamiya A, Kakinuma S, Zeniya M, Nishinakamura R, Tajiri H, et al. Sall4 regulates cell fate decision in fetal hepatic stem/progenitor cells. Gastroenterology 2009;136:1000–1011.
[12] Sher F, Roßler R, Brouwer N, Balasubramaniyan V, Boddeke E, Copray S. Differentiation of neural stem cells into oligodendrocytes: involvement of the polycomb group protein Ezh2. Stem Cells 2008;26:2875–2883.
[13] Ezhkova E, Pasolli HA, Parker JS, Stokes N, Su IH, Hannon G, et al. Ezh2 orchestrates gene expression for the stepwise differentiation of tissue-specific stem cells. Cell 2009;136:1122–1135.
[14] Oguro H, Iwama A, Morita Y, Kamijo T, van Lohuizen M, Nakauchi H. Differential impact of *Ink4a* and *Arf* on hematopoietic stem cells and their bone marrow microenvironment in *Bmi1*-deficient mice. J Exp Med 2006;203:2247–2253.
[15] Molofsky AV, He S, Bydon M, Morrison SJ, Pardal R. Bmi-1 promotes neural stem cell self-renewal and neural development but not mouse growth and survival by repressing the $p16^{Ink4a}$ and $p19^{Arf}$ senescence pathways. Genes Dev 2005;19:1432–1437.
[16] Bracken AP, Kleine-Kohlbrecher D, Dietrich N, Pasini D, Gargiulo G, Beekman C, et al. The Polycomb group proteins bind throughout the INK4A–ARF locus and are disassociated in senescent cells. Genes Dev 2007;21:525–530.
[17] Bernstein BE, Mikkelsen TS, Xie X, Kamal M, Huebert DJ, Cuff J, et al. A bivalent chromatin structure marks key developmental genes in embryonic stem cells. Cell 2006;125:315–326.
[18] Ku M, Koche RP, Rheinbay E, Mendenhall EM, Endoh M, Mikkelsen TS, et al. Genomewide analysis of PRC1 and PRC2 occupancy identifies two classes of bivalent domains. PLoS Genet 2008;4:e1000242.
[19] Pietersen AM, Horlings HM, Hauptmann M, Langerød A, Ajouaou A, Cornelissen-Steijger P, et al. EZH2 and BMI1 inversely correlate with prognosis and TP53 mutation in breast cancer. Breast Cancer Res 2008;10:R109.
[20] Chen H, Gu X, Su IH, Bottino R, Contreras JL, Tarakhovsky A, et al. Polycomb protein Ezh2 regulates pancreatic beta-cell Ink4a/Arf expression and regeneration in diabetes mellitus. Genes Dev 2009;23:975–985.
[21] Sasaki M, Yamaguchi J, Itatsu K, Ikeda H, Nakanuma Y. Over-expression of polycomb group protein EZH2 relates to decreased expression of p16 INK4a in cholangiocarcinogenesis in hepatolithiasis. J Pathol 2008;215: 175–183.
[22] Nagy P, Bisgaard HC, Thorgeirsson SS. Expression of hepatic transcription factors during liver development and oval cell differentiation. J Cell Biol 1994;126:223–233.
[23] Sund NJ, Ang SL, Sackett SD, Shen W, Daigle N, Magnuson MA, et al. Hepatocyte nuclear factor 3b (Foxa2) is dispensable for maintaining the differentiated state of the adult hepatocyte. Mol Cell Biol 2000;20: 5175–5183.
[24] Ishizaka S, Shiroi A, Kanda S, Yoshikawa M, Tsujinoue H, Kuriyama S, et al. Development of hepatocytes from ES cells after transfection with the HNF-3beta gene. FASEB J 2002;16:1444–1446.
[25] Ishii K, Yoshida Y, Akechi Y, Sakabe T, Nishio R, Ikeda R, et al. Hepatic differentiation of human bone marrow-derived mesenchymal stem cells by tetracycline-regulated hepatocyte nuclear factor 3beta. Hepatology 2008;48:597–606.
[26] Tan EH, Ma FJ, Gopinadhan S, Sakban RB, Wang ND. C/EBP alpha knock-in hepatocytes exhibit increased albumin secretion and urea production. Cell Tissue Res 2007;330:427–435.
[27] Zaret KS. Regulatory phases of early liver development: paradigms of organogenesis. Nat Rev Genet 2002;3:499–512.
[28] Boyer LA, Plath K, Zeitlinger J, Brambrink T, Medeiros LA, Lee TI, et al. Polycomb complexes repress developmental regulators in embryonic stem cells. Nature 2006;441:349–353.
[29] Kuzmichev A, Margueron R, Vaquero A, Preissner TS, Scher M, Kirmizis A, et al. Composition and histone substrates of polycomb repressive group complexes change during cellular differentiation. Proc Natl Acad Sci USA 2005;102:1859–1864.

Scandinavian Journal of Gastroenterology, 2010; 45: 243–249

informa
healthcare

ORIGINAL ARTICLE

Risk of Hepatocellular Carcinoma in Patients with Chronic Hepatitis B Virus Infection

KENICHI ITO[1], MAKOTO ARAI[1], FUMIO IMAZEKI[1], YUTAKA YONEMITSU[1], DAN BEKKU[1], TATSUO KANDA[1], KEIICHI FUJIWARA[1], KENICHI FUKAI[1], KENICHI SATO[2], SAKAE ITOGA[2], FUMIO NOMURA[2] & OSAMU YOKOSUKA[1]

[1]*Departments of Medicine and Clinical Oncology, and* [2]*Departments of Molecular Diagnosis, Graduate School of Medicine, Chiba University, Chiba, Japan*

Abstract

Objective. To determine the risk factors for the occurrence of hepatocellular carcinoma (HCC) in patients with hepatitis B virus (HBV) infection. ***Material and methods.*** A total of 620 patients who tested positive for hepatitis B surface antigen and were referred to Chiba University Hospital between February 1985 and March 2008 were included in the study and the following characteristics were analyzed: age, gender, status of hepatitis B e antigen, alanine aminotransferase level, HBV DNA level, and number of platelets (PLTs). ***Results.*** HCC was detected in 30 cases during the follow-up period (5.4 ± 5.1 years). Multivariate analysis revealed that age >40 years [compared with patients aged <40 years; odds ratio (OR) = 4.28; 95% confidence interval (CI) = 1.68–10.9] and PLT level <206,000/μl (compared with patients with a higher PLT level; OR = 8.50; 95% CI = 1.98–36.2) were predictive factors for HCC occurrence. In patients aged >40 years, the HBV DNA level (compared with <5.0 log copies/ml; OR = 4.22, 95% CI = 1.13–15.8) and PLT level (compared with patients with >196,000/μl PLTs; OR = 15.6, 95% CI = 2.06–118.3) were predictive factors for HCC occurrence. ***Conclusions.*** Advanced age and low PLT level were risk factors for HCC occurrence in patients with HBV infection. In patients aged >40 years, viral load was also a risk factor for HCC.

Key Words: *Hepatitis B virus, hepatocellular carcinoma*

Introduction

The clinical course of patients with hepatitis B virus (HBV) infection varies considerably [1]. Therefore, long-term follow-up studies of patients with HBV infection are quite complex and difficult. In most of the patients, the disease is either non-progressive or shows a slow progression and is usually accompanied by the loss of serum HBV DNA after seroconversion of hepatitis B e antigen (HBeAg) [2]. Some patients show continuous elevation of the alanine aminotransferase (ALT) level, which leads to cirrhosis [3]. HBV infection is also associated with an increased risk of developing hepatocellular carcinoma (HCC), which is one of the most common human cancers and causes of death. Although previous studies have attempted to determine factors influencing the prognosis of patients with HBV infection, the key factors remain to be identified. Recent studies have indicated that the serum level of HBV DNA correlates with the progression of liver diseases [1,4–6]. However, viral load alone cannot predict the occurrence of HCC in the future [7]. In this study, multivariate analyses of the risk factors for HCC occurrence were performed for data obtained from 620 patients with HBV infection who were referred to a single institute in Japan.

Correspondence: Makoto Arai, MD, Department of Medicine and Clinical Oncology (K1), Graduate School of Medicine, Chiba University, Inohana 1-8-1, Chiba-City, 260-8670, Japan. Tel: +81-43-226-2083. Fax: +81-43-226-2088. E-mail: araim-cib@umin.ac.jp

(Received 15 September 2009; accepted 27 October 2009)

ISSN 0036-5521 print/ISSN 1502-7708 online
DOI: 10.3109/00365520903450113

Material and methods

Patients

This was a retrospective analysis. The study was approved by the ethical committee of Chiba University and written informed consent was obtained from all the patients. Of the hepatitis B surface antigen (HBsAg)-positive carriers ($n = 676$) who were referred to Chiba University Hospital between February 1985 and March 2008, those who tested positive for hepatitis C virus (HCV) antibody (anti-HCV) or had autoimmune liver disease and those who had another potential cause of chronic liver disease were excluded. The characteristics of the excluded HBsAg-positive carriers were as follows: anti-HCV positivity in 12, autoimmune liver disease in four and primary biliary cirrhosis in one. Five patients who had previously received lamivudine treatment were also excluded. Thirty-nine patients consulted a physician only once and were excluded from further analysis. Thus, a total of 620 patients were further analyzed. Serum samples were collected during diagnosis and stored at –20°C until analysis.

Serologic markers, HBV DNA quantitative assay, and genotyping

HBsAg, HBeAg, and anti-HBe levels were determined by enzyme-linked immunosorbent assay (ELISA; Abbott Laboratories, Chicago, IL) and anti-HCV was also measured by ELISA (Ortho Diagnostics, Tokyo, Japan). Serum HBV DNA levels were quantified by polymerase chain reaction (PCR) assay (Amplicor HBV Monitor; Roche Diagnostics, Basle, Switzerland); the linear range of this assay was 2.6–7.6 log copies (LC)/ml. The six major genotypes of HBV (A–F) were determined by EIA (HBV Genotype EIA; Institute of Immunology Co., Ltd., Tokyo, Japan). Aspartate aminotransferase (AST), ALT, and the number of platelets were determined and the aminotransferase to platelet ratio index (APRI) was calculated [8].

Statistical analysis

The baseline data are presented as mean ± SD. The difference in the values of clinical parameters between the two groups was analyzed by unpaired t-test, Welch's t-test, and chi-square test. The Cox proportional hazards model was used to identify factors predictive of HCC occurrence using the SPSS version 16.1 software package (SPSS Inc., Chicago, IL).

Results

Demographic characteristics of HCC and control patients

None of the study participants had HCC at entry. In total, 30 incident HCC cases (HCC group) occurred during the follow-up period. During the follow-up period, most of the patients were re-evaluated at least once a year for liver function and detection of HCC. Screening for detection of HCC was performed on the basis of typical findings of abdominal ultrasonography, dynamic CT, angiography, and/or MRI. For all patients suspected of having HCC by imaging analysis, the diagnosis of HCC was confirmed by pathological analysis. If the patient had HCC or was being treated with an antiviral drug (lamivudine or entecavir), we terminated the follow-up. At baseline, significant differences were observed in age, gender, status of HBeAg, ALT and HBV DNA levels, number of platelets (PLTs), and APRI between the HCC ($n = 30$) and control ($n = 590$) groups (Table I). The 590 patients in whom HCC was not detected during the follow-up period constituted the control group. The average follow-up period was 5.1 ± 4.1 and 5.4 ± 5.2 years in the HCC and control groups, respectively, and this difference was not significant.

Patients with HBV

The differences in age, sex, PLT and ALT levels, status of HBeAg, and HBV DNA level between the HCC and control groups were investigated. We defined threshold levels as age 40 years, HBV DNA 5.3 LC/ml, ALT 72.9 IU/l, and PLTs 206,000/μl according to the average data of all patients. Univariate analysis revealed that age, number of PLTs, and HBV DNA level at baseline were predictive factors for HCC occurrence. Multivariate analysis revealed that age >40 years [compared with patients aged <40 years; odds ratio (OR) = 4.28; 95% confidence interval (CI) = 1.68–10.9] and PLT level <206,000/μl (compared with patients with a higher PLT level; OR = 8.50, 95% CI = 1.98–36.2) were predictive factors for HCC occurrence (Table II). Thus, these analyses revealed that age and PLT level were the most important factors influencing future occurrence of HCC. Kaplan–Meier curves were constructed for age ($P < 0.0001$; log-rank test; Figure 1a), PLT level ($P < 0.0001$; log-rank test; Figure 1b), and HBV DNA (P = NS; log-rank test; Figure 1c). Next, we categorized the HBV patients into two subgroups according to the thresholds of age and PLT level based on the average data, and performed further analysis. Because there was only one HCC patient aged <40 years and

Table I. Characteristics of study subjects and their association with HCC.

Parameter	Group			*P*
	Total	HCC	Controls	
No. of patients	620	30	590	
Gender; *n* (%)				<0.001[a]
Male	364 (59)	20 (67)	344 (58)	
Female	256 (41)	10 (33)	246 (42)	
Age (years); mean ± SD	40.0 ± 14.2	50.0 ± 11.6	40.0 ± 14.2	<0.001[b]
HBeAg status; *n* (%)				<0.001[a]
Positive	269 (43)	17 (57)	252 (43)	
Negative	351 (57)	13 (43)	338 (57)	
HBV DNA (LC/mL); mean ± SD	5.3 ± 2.0	6.4 ± 1.3	5.3 ± 2.0	0.002[b]
ALT (IU/l); mean ± SD	72.9 ± 89.3	105.0 ± 129.3	71.0 ± 86.6	0.041[c]
PLTs (/μl); mean ± SD	206,000 ± 66,000	130,000 ± 51,160	210,000 ± 64,410	<0.001[c]
APRI > 0.5; *n* (%)	294 (47.4)	27 (90)	267 (45.3)	<0.001[a]
Interval between two consecutive visits (years); mean ± SD	5.4 ± 5.1	5.1 ± 4.1	5.4 ± 5.2	NS[c]
Genotype A/B/C/D/not determined; *n*	7/38/333/0/242	1/0/24/0/5	6/38/309/0/237	NS[a]

[a]Chi-square test.
[b]Welch's *t*-test.
[c]Unpaired *t*-test.

only two cases had a PLT level > 206,000/μl, we did not analyze these groups.

Analysis of the subgroup of HBV patients aged > 40 years

HCC was detected in 29 patients in the group aged >40 years (n = 372). Significant differences were observed in the status of HBeAg, HBV DNA, and PLT levels at baseline between the HCC (n = 29) and control groups (n = 343). The average follow-up period was 5.1 ± 4.1 and 5.0 ± 4.7 years in the HCC and control groups, respectively, and this difference was not significant. We defined thresholds as age 49 years, HBV DNA 5.0 LC/ml, ALT 66.0 IU/l, and PLTs 196,000/μl, according to the average data for the patients aged >40 years. The risk factors for HCC occurrence in patients aged >40 years were analyzed by Cox regression analysis. Univariate analysis revealed that ALT, PLT, and HBV DNA levels at baseline were predictive factors for HCC occurrence. Multivariate analysis revealed that the HBV DNA

Table II. Multivariate analysis of risk factors associated with HCC in patients with HBV infection.

Risk factor	All patients[a]		Patients aged >40 years[b]		Patients with PLTs <206,000 /μl[c]	
	HR (95% CI)	*P*	HR (95% CI)	*P*	HR (95% CI)	*P*
Age	4.28 (1.68–10.9)	0.002	2.16 (0.88–5.29)	NS	1.75 (0.71–4.34)	NS
Male gender	1.48 (0.67–3.26)	NS	2.25 (0.86–5.90)	NS	1.43 (0.61–3.35)	NS
HBeAg-positive	1.34 (0.59–3.06)	NS	0.98 (0.41–2.33)	NS	1.06 (0.45–2.51)	NS
HBV-DNA	1.59 (0.62–4.13)	NS	4.22 (1.13–15.8)	0.032	1.20 (0.49–2.94)	NS
ALT	0.86 (0.40–1.87)	NS	1.44 (0.61–3.44)	NS	0.923 (0.40–2.11)	NS
PLTs	8.50 (1.98–36.2)	0.004	15.6 (2.06–118.3)	0.008	4.49 (1.62–12.5)	0.004

[a]The thresholds of age, HBV-DNA, ALT, and PLTs were defined as 40 years, 5.3 LC/ml, 72.9 IU/l, and 206,000 /μl, respectively.
[b]The thresholds of age, HBV-DNA, ALT, and PLTs were defined as 49 years, 5.0 LC /ml, 66.0 IU/l, and 196,000 /μl, respectively.
[c]The thresholds of age, HBV-DNA, ALT, and PLTs were defined as 42 years, 5.8 LC /ml, 84 IU/l, and 159,000 /μl, respectively.
HR = hazard ratio.

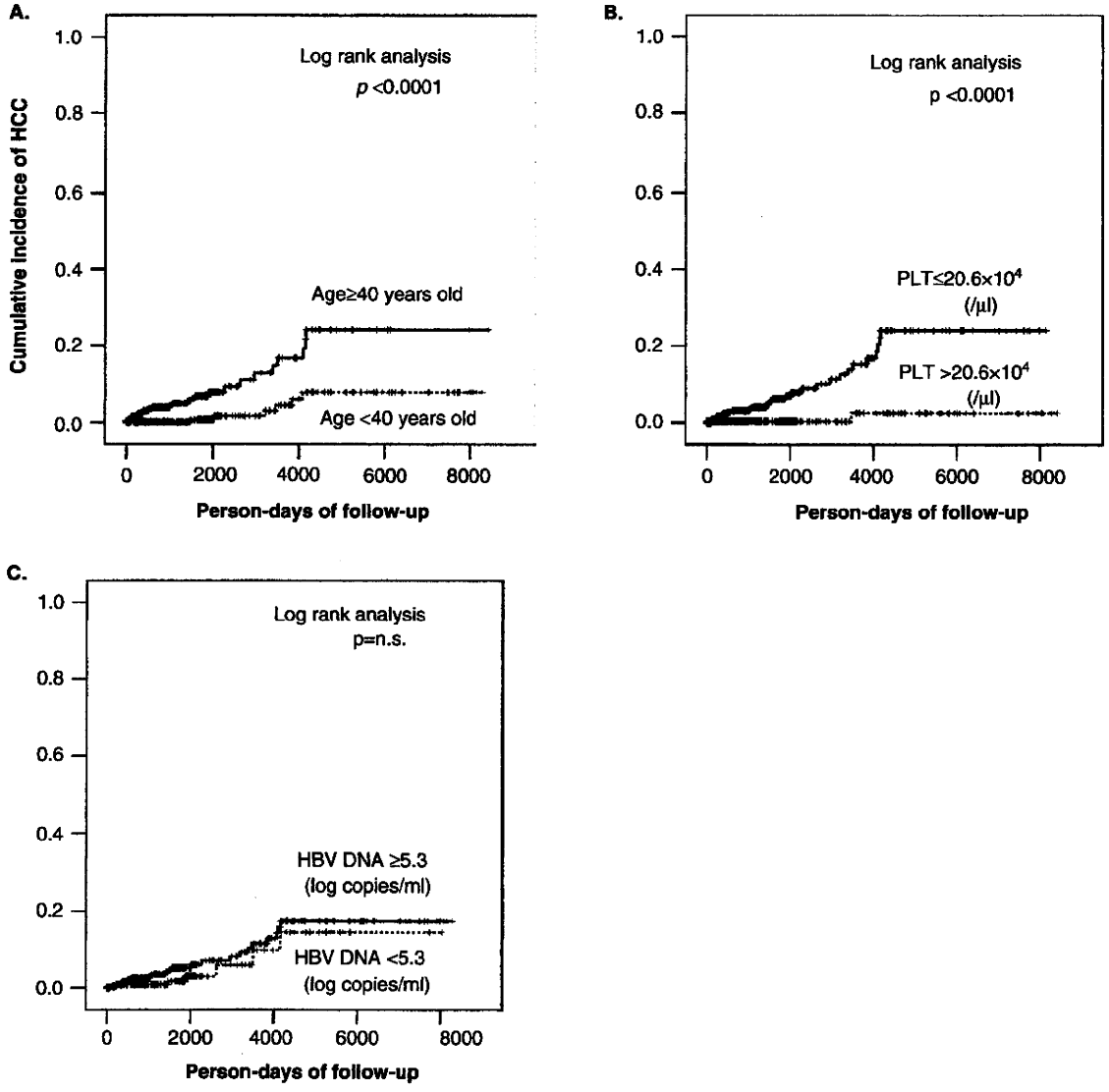

Figure 1. Cumulative occurrence of HCC based on (a) number of PLTs, (b) age, and (c) HBV DNA level. Thresholds for age, number of PLTs, and HBV DNA level were defined according to the average data for all patients. Dotted lines indicate the control group (high number of PLTs, younger age, and low HBV DNA level).

level (compared with <5.0 LC/ml; OR = 4.22; 95% CI = 1.13–15.8) and PLT level (compared with >196,000/μl; OR = 15.6; 95% CI = 2.06–118.3) were predictive factors for HCC occurrence (Table II). Kaplan–Meier curves were constructed for HBV DNA (P = 0.001; log-rank test; Figure 2).

Analysis of the subgroup of HBV patients with PLTs <206,000/μl

HCC was detected in 28 patients in the group with PLTs <206,000/μl (n = 329). The risk factors for HCC occurrence in the group with <206,000/μl PLTs were analyzed by Cox regression analysis. Univariate analysis revealed that age and PLT level at baseline were predictive factors for HCC occurrence. Multivariate analysis revealed that PLT level (compared with patients with >159,000/μl; OR = 4.49; 95% CI = 1.62–12.5) was the only predictive factor for HCC occurrence (Table II).

Discussion

In Japan, HBV infection is one of the most important factors determining HCC occurrence [9]. Moreover, HCC is one of the most important determinants for

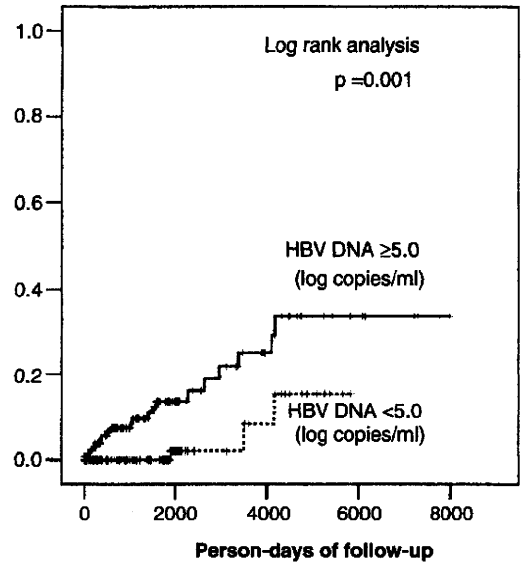

Figure 2. Cumulative occurrence of HCC based on the HBV DNA level in patients aged > 40 years. The threshold for the HBV DNA level was defined according to the average data for the patients aged > 40 years. A significant difference was observed by log-rank test. The dotted line indicates the control group (low HBV DNA level).

the prognosis of patients with HBV infection. In previous studies, factors associated with an increased risk of HCC among people with chronic HBV infection included demographic characteristics, lifestyle, and environmental, viral and clinical factors. Among these, male gender, older age, HBV genotype, cirrhosis, elevated ALT, and high viral load were found to be factors associated with HCC [6,10–19]. We focused on clinical factors which may be tested easily and for which tests are available all over the world. This report clarifies the relative risk for HCC in all patients with HBV who were referred to a single institute in Japan and provides important information for physicians.

In this study, the relative risk of HCC was found to be increased to 4.28 (95% CI 1.68–10.9) times higher for patients aged > 40 years compared with those aged < 40 years. In addition, a low PLT level, which indicates advanced fibrosis in the liver, including cirrhosis, was a risk factor for HCC: the relative risk was found to be increased to 8.50 (95% CI 1.98–36.2) times higher for patients with a PLT level < 206,000/μl compared with higher levels. The HBV DNA level was not selected as a risk factor for HCC occurrence in all patients with HBV infection by multivariate analysis. Previous follow-up studies have shown that viral load is an important and independent factor for HCC occurrence [4,5,20]. However, in the present study, although various thresholds of HBV DNA level were used for analysis, none of the thresholds showed statistical significance in multivariate analysis (data not shown). In contrast, the analysis intended for patients aged > 40 years revealed that high HBV viral load was added as a risk factor for HCC. By changing the threshold of HBV DNA from 4.5 to 5.3 LC/ml in 0.1-log increments, 5.0 or 5.1 LC/ml were found to be the best (data not shown); therefore we designated the threshold of HBV DNA level as > 5.0 LC/ml. In our study, HBV carriers aged > 40 years with HBV DNA levels > 5.0 LC/ml had a 4.22-times higher risk of HCC compared to HBV carriers with lower viral loads. In previous studies in Japan regarding predictive factors for HCC, Ohata et al. [5] reported that age, HBV DNA, and staging of fibrosis were the important factors, while Murata et al. [21] reported that the number of PLTs was the only factor after HBeAg seroconversion. On the other hand, in an analysis of patients with liver cirrhosis in Japan, levels of HBV DNA and/or ALT were the predictive factors for HCC [12,19]. Taken together with the present study, these reports suggest that the HBV DNA level may not be an absolute factor for predicting HCC in the analysis, irrespective of the age of the patients and the number of PLTs, but that in patients with advanced age or low numbers of PLTs, indicating advanced fibrosis of the liver, HBV DNA could be a predictive factor for the occurrence of HCC. The PLT level negatively reflects the extent of liver fibrosis [22], therefore it is very difficult to achieve an improvement in liver fibrosis and to recover the PLT level concomitantly, but a high viral load can be lowered by antiviral drug treatment. Therefore, in patients aged > 40 years, lowering the viral load using an antiviral drug might be an important way to avoid the occurrence of HCC but, in younger patients, lowering the HBV DNA level may not result in direct inhibition of HCC occurrence, although the activity of hepatitis could be suppressed.

The decrease in the number of PLTs in patients with liver disease reflects advanced fibrosis of the liver, which is strongly related to HCC occurrence. In fact, the patients in the HCC group of our study were suggested to show advanced fibrosis because they had higher values of APRI than the controls. In addition to being a marker of liver fibrosis, the influence of PLTs on cytotoxic T lymphocytes (CTLs) has been studied with keen interest. Chronic HBV infection is characterized by an inefficient CTL response, which often results in continuous destruction of hepatocytes. A recent study indicated that PLTs are required for virus-specific CTLs to accumulate within the liver and perform pathogenetic and/or antiviral roles [23]. In our study, low PLT number was a strong risk factor for HCC in all the HBV carriers, irrespective of age or PLT number at baseline. Especially in the HBV

carriers aged > 40 years, low PLT number has the strongest association with HCC occurrence. Therefore, older HBV carriers with low PLT levels should be followed closely because of a high possibility of HCC occurrence, as for HCV carriers with low PLT levels [24].

The presence of HBeAg is often associated with active liver disease, whereas HBeAg seroconversion often coincides with loss of HBV DNA in serum, normalization of the ALT level, and clinical remission [25]. Spontaneous HBeAg seroconversion confers a good long-term outcome on most patients. In this study, the status of HBeAg at baseline differed significantly between the HCC and control groups; however, the status of HBeAg was not identified by univariate analysis as a predictive factor for HCC occurrence. From these results, we speculated that the HBe protein was not the direct precursor of HCC, although the HBe antigen status often reflects the replication of HBV DNA.

In this study, we evaluated parameters for predicting HCC only at first admission. A previous study reported that changes in ALT or HBV DNA levels during the follow-up period were important for predicting advanced liver disease and HCC [26]. We need to evaluate the importance of following changes in these parameters.

There was only one HCC patient aged < 40 years. This patient was male and was followed up from the age of 27 years; his ALT, HBV DNA, and PLT levels and the status of HBeAg at baseline were 34 IU/l, 7.7 LC/ml, 203,000/μl, and positive, respectively. It was difficult to predict the occurrence of HCC in this case only on the basis of the risk factors for HCC indicated in this study. Hence, we need to find an adequate risk factor to predict HCC in such a case.

In conclusion, advanced age and low PLT level were the risk factors for HCC in patients with HBV infection, irrespective of the PLT level at baseline. In patients aged > 40 years, viral load was added as a risk factor for HCC.

Declaration of interests: The authors indicated no potential conflict of interest.

References

[1] Yang HI, Yeh SH, Chen PJ, Iloeje UH, Jen CL, Su J, et al. Associations between hepatitis B virus genotype and mutants and the risk of hepatocellular carcinoma. J Natl Cancer Inst 2008;100:1134–43.

[2] Chu CJ, Hussain M, Lok AS. Quantitative serum HBV DNA levels during different stages of chronic hepatitis B infection. Hepatology 2002;36:1408–15.

[3] Fujiwara A, Sakaguchi K, Fujioka S, Iwasaki Y, Senoh T, Nishimura M, et al. Fibrosis progression rates between chronic hepatitis B and C patients with elevated alanine aminotransferase levels. J Gastroenterol 2008;43:484–91.

[4] Chen CJ, Yang HI, Su J, Jen CL, You SL, Lu SN, et al. Risk of hepatocellular carcinoma across a biological gradient of serum hepatitis B virus DNA level. JAMA 2006;295:65–73.

[5] Ohata K, Hamasaki K, Toriyama K, Ishikawa H, Nakao K, Eguchi K. High viral load is a risk factor for hepatocellular carcinoma in patients with chronic hepatitis B virus infection. J Gastroenterol Hepatol 2004;19:670–5.

[6] Wu CF, Yu MW, Lin CL, Liu CJ, Shih WL, Tsai KS, et al. Long-term tracking of hepatitis B viral load and the relationship with risk for hepatocellular carcinoma in men. Carcinogenesis 2008;29:106–12.

[7] Yuen MF, Tanaka Y, Fong DY, Fung J, Wong DK, Yuen JC, et al. Independent risk factors and predictive score for the development of hepatocellular carcinoma in chronic hepatitis B. J Hepatol 2009;50:80–8.

[8] Shaheen AA, Myers RP. Diagnostic accuracy of the aspartate aminotransferase-to-platelet ratio index for the prediction of hepatitis C-related fibrosis: a systematic review. Hepatology 2007;46:912–21.

[9] Befeler AS, Di Bisceglie AM. Hepatocellular carcinoma: diagnosis and treatment. Gastroenterology 2002;122: 1609–19.

[10] Liu CJ, Chen BF, Chen PJ, Lai MY, Huang WL, Kao JH, et al. Role of hepatitis B viral load and basal core promoter mutation in hepatocellular carcinoma in hepatitis B carriers. J Infect Dis 2006;193:1258–65.

[11] Yu MW, Hsu FC, Sheen IS, Chu CM, Lin DY, Chen CJ, et al. Prospective study of hepatocellular carcinoma and liver cirrhosis in asymptomatic chronic hepatitis B virus carriers. Am J Epidemiol 1997;145:1039–47.

[12] Mahmood S, Niiyama G, Kamei A, Izumi A, Nakata K, Ikeda H, et al. Influence of viral load and genotype in the progression of Hepatitis B-associated liver cirrhosis to hepatocellular carcinoma. Liver Int 2005;25:220–5.

[13] Sumi H, Yokosuka O, Seki N, Arai M, Imazeki F, Kurihara T, et al. Influence of hepatitis B virus genotypes on the progression of chronic type B liver disease. Hepatology 2003;37:19–26.

[14] Fattovich G, Stroffolini T, Zagni I, Donato F. Hepatocellular carcinoma in cirrhosis: incidence and risk factors. Gastroenterology 2004;127:S35–50.

[15] Park BK, Park YN, Ahn SH, Lee KS, Chon CY, Moon YM, et al. Long-term outcome of chronic hepatitis B based on histological grade and stage. J Gastroenterol Hepatol 2007;22:383–8.

[16] Chen CJ, Liang KY, Chang AS, Chang YC, Lu SN, Liaw YF, et al. Effects of hepatitis B virus, alcohol drinking, cigarette smoking and familial tendency on hepatocellular carcinoma. Hepatology 1991;13:398–406.

[17] McMahon BJ, Holck P, Bulkow L, Snowball M. Serologic and clinical outcomes of 1536 Alaska Natives chronically infected with hepatitis B virus. Ann Intern Med 2001;135:759–68.

[18] Tang B, Kruger WD, Chen G, Shen F, Lin WY, Mboup S, et al. Hepatitis B viremia is associated with increased risk of hepatocellular carcinoma in chronic carriers. J Med Virol 2004;72:35–40.

[19] Ishikawa T, Ichida T, Yamagiwa S, Sugahara S, Uehara K, Okoshi S, et al. High viral loads, serum alanine aminotransferase and gender are predictive factors for the development

of hepatocellular carcinoma from viral compensated liver cirrhosis. J Gastroenterol Hepatol 2001;16:1274–81.

[20] Kumar M, Kumar R, Hissar SS, Saraswat MK, Sharma BC, Sakhuja P, et al. Risk factors analysis for hepatocellular carcinoma in patients with and without cirrhosis: a case–control study of 213 hepatocellular carcinoma patients from India. J Gastroenterol Hepatol 2007;22:1104–11.

[21] Murata K, Sugimoto K, Shiraki K, Nakano T. Relative predictive factors for hepatocellular carcinoma after HBeAg seroconversion in HBV infection. World J Gastroenterol 2005;11:6848–52.

[22] Karasu Z, Tekin F, Ersoz G, Gunsar F, Batur Y, Ilter T, et al. Liver fibrosis is associated with decreased peripheral platelet count in patients with chronic hepatitis B and C. Dig Dis Sci 2007;52:1535–9.

[23] Iannacone M, Sitia G, Isogawa M, Marchese P, Castro MG, Lowenstein PR, et al. Platelets mediate cytotoxic T lymphocyte-induced liver damage. Nat Med 2005;11:1167–9.

[24] Lok AS, Seeff LB, Morgan TR, di Bisceglie AM, Sterling RK, Curto TM, et al. Incidence of hepatocellular carcinoma and associated risk factors in hepatitis C-related advanced liver disease. Gastroenterology 2009;136:138–48.

[25] Ma H, Wei L, Guo F, Zhu S, Sun Y, Wang H. Clinical features and survival in Chinese patients with hepatitis B e antigen-negative hepatitis B virus-related cirrhosis. J Gastroenterol Hepatol 2008;23:1250–8.

[26] Ikeda K, Arase Y, Kobayashi M, Someya T, Hosaka T, Saitoh S, et al. Hepatitis B virus-related hepatocellular carcinogenesis and its prevention. Intervirology 2005;48: 29–38.

European Journal of Radiology 75 (2010) e102–e106

Contents lists available at ScienceDirect

European Journal of Radiology

journal homepage: www.elsevier.com/locate/ejrad

Changes in tumor vascularity precede microbubble contrast accumulation deficit in the process of dedifferentiation of hepatocellular carcinoma

Hitoshi Maruyama*, Masanori Takahashi, Hiroyuki Ishibashi, Shinichiro Okabe, Masaharu Yoshikawa, Osamu Yokosuka

Department of Medicine and Clinical Oncology, Chiba University Graduate School of Medicine 1-8-1, Inohana, Chuou-ku, Chiba 260-8670, Japan

ARTICLE INFO

Article history:
Received 19 June 2009
Received in revised form 22 August 2009
Accepted 25 August 2009

Keywords:
Ultrasound
Hepatocellular carcinoma
Contrast agent
Sonazoid
Nodule-in-nodule

ABSTRACT

Purpose: To elucidate the changes in tumor vascularity and microbubble accumulation on contrast-enhanced sonograms, in relation to the dedifferentiation of hepatocellular carcinoma (HCC).
Materials and methods: This prospective study enrolled 10 patients with histologically proven HCC (14.4–39.0 mm, 26.1 ± 7.4) showing nodule-in-nodule appearance upon contrast-enhanced computed tomography. Contrast-enhanced ultrasound was performed by harmonic imaging under a low mechanical index (0.22–0.25) during the vascular phase (agent injection to 1 min) and late phase (15 min) following the injection of Sonazoid™ (0.0075 ml/kg). Contrast enhancement in the inner and outer nodules was assessed in comparison with that in adjacent liver parenchyma as hyper-, iso-, or hypo-enhanced.
Results: Vascular-phase enhancement of all 10 inner nodules was hyper-enhanced, and that of outer nodules was hyper-enhanced in 3, iso-enhanced in 2, and hypo-enhanced in 5. Late-phase enhancement of inner nodules was hypo-enhanced in 8 and iso-enhanced in 2. Furthermore, late-phase enhancement of outer nodules was iso-enhanced in the 7 lesions that showed iso- or hypo-enhancement in the vascular phase, and hypo-enhanced in the 3 with hyper-enhancement in the vascular phase. Late-phase hypo-enhancement was significantly more frequent in the nodules showing early-phase hyper-enhancement (11/13) than in the nodules showing early-phase iso- or hypo-enhancement (0/7) in both the inner and outer nodules.
Conclusion: Dedifferentiation of HCC may be accompanied by changes in tumor vascularity prior to a reduction in microbubble accumulation. Observation of the vascular phase may be more useful than late-phase imaging for the early recognition of HCC dedifferentiation when using contrast-enhanced ultrasound with Sonazoid.

1. Introduction

Hepatocellular carcinoma (HCC) is one of the most common malignancies, and its incidence is increasing worldwide, especially in the eastern part of Asia [1,2]. The diagnosis of HCC is an issue of critical importance, in part because the prognosis of patients with cirrhosis depends to a large extent on the occurrence and progression of this neoplasm. Considering the limitations of tumor markers such as alpha fetoprotein (AFP) for HCC surveillance, it is necessary to have easy access to imaging examinations for cirrhotic patients [3,4].

Intra-tumor vascularity changes during the multistep process of carcinogenesis in HCC, including the presence of numerous tumor vessels, as well as a paucity of Kupffer cells comprise the well-known pathological appearance that is characteristic of HCC [5–7]. However, some well-differentiated HCCs have a hypo- or iso-vascular appearance, along with Kupffer cells distributed within the tumor nodule [6,7]. The relationship between the changes in tumor vascularity and Kupffer cell distribution, in accordance with the dedifferentiation process of HCC, has not been fully addressed in previous studies.

Contrast-enhanced ultrasound (US) has become popular as a non-invasive diagnostic tool for assessing focal hepatic lesions, due to the recent advances in digital technology incorporated into US equipment [8–10]. Microbubble contrast agents can be divided into two classes based on whether they do or do not accumulate in the liver, and both Levovist® (Schering, Berlin, Germany) and Sonazoid™ (GE Healthcare, Oslo, Norway) are classified as the former. They provide images of static microbubbles, which appear to demonstrate the function of the reticuloendothelial system such as phagocytosis by Kupffer cells, as well as imaging dynamic microbubbles that depict the hemodynamic circulation [11–14]. Therefore, contrast-enhanced US with these microbubble

* Corresponding author. Tel.: +81 43 2262083; fax: +81 43 2262088.
E-mail addresses: maru-cib@umin.ac.jp (H. Maruyama), machat@aa.pial.jp (M. Takahashi), bashiish@yahoo.co.jp (H. Ishibashi), okabeshin1966@yahoo.co.jp (S. Okabe), yoshikawa@faculty.chiba-u.jp (M. Yoshikawa), yokosukao@faculty.chiba-u.jp (O. Yokosuka).

0720-048X/$ – see front matter © 2009 Elsevier Ireland Ltd. All rights reserved.
doi:10.1016/j.ejrad.2009.08.017

contrast agents may reveal both tumor vascularity and Kupffer cell distribution in HCC lesions.

The nodule-in-nodule appearance of HCCs is a pattern that reflects cell dedifferentiation, because tumor elements with varying degrees of differentiation coexist in a single mass [15–20]. Assessment of contrast-enhanced US findings in HCCs with nodule-in-nodule appearance may reveal the dedifferentiation-related changes involved with tumor neovascularity and Kupffer cell distribution in these HCC lesions [21]. Against this background, we examined differences in contrast enhancement between the inner and outer nodules in HCC lesions having a nodule-in-nodule appearance. The purpose of this study was to elucidate the changes in tumor vascularity and microbubble accumulation exhibited on contrast-enhanced sonograms, in relation to the dedifferentiation of HCC.

2. Patients and methods

2.1. Patients

During the period from July 2007 to February 2009, a prospective study approved by the Ethics Committee of Chiba University Hospital, Chiba, Japan, was performed to examine Sonazoid-induced enhancement on sonograms of patients with HCC, after obtaining their informed written consent. A total of 513 patients with HCC underwent both contrast-enhanced computed tomography (CT) and contrast-enhanced US examination during this time period. There were 10 consecutive patients with HCC showing a nodule-in-nodule appearance upon contrast-enhanced CT, specifically, an inner nodule with hypervascularity and an outer nodule with a hypo-, iso-, or slightly hypervascular appearance on the images in the hepatic artery-dominant phase. The study enrolled these 10 cirrhotic patients as subjects, with all their HCC lesions proven histologically. The study patients consisted of 5 males and 5 females, with a mean age ± standard deviation (SD) of 67.3 ± 8.9 years (range 45–78 years). The diagnosis of liver cirrhosis was based on imaging findings, along with clinical symptoms and biochemistry results in all 10 patients; 9 of the patients were positive for hepatitis C virus antibody, and one patient was positive for hepatitis B virus surface antigen.

Each patient had one HCC tumor mass with a nodule-in-nodule appearance and a maximum diameter ranging from 14.4 to 39.0 mm (mean 26.1 ± 7.4 mm) on the sonogram. The serum AFP level ranged from 3.4 to 1266.1 ng/ml, with normal values (<20 ng/ml) found in 6 patients and abnormal values in 4 patients. No patients had egg allergy, which is a contraindication to the use of Sonazoid.

2.2. US examination

US examination was performed using the SSA-790A system (Aplio XG; Toshiba Medical Systems, Tokyo, Japan) with a 3.75-MHz convex probe. All patients underwent US examination after a fast of more than 4 h. At first, non-contrast grey-scale US (tissue harmonic imaging, 2.5/5.0 MHz, 14–27 Hz) was performed to observe the tumor appearance, to measure the diameters of the inner and outer nodules, and to select the scan plane allowing the most stable observation for contrast-enhanced US. Subsequently, color Doppler US was used to check for the presence or absence of vascular abnormality, such as arterio-portal communication, portal vein thrombosis, and/or portal vein tumor thrombosis. Next, the settings of the US system were changed for contrast-enhanced US, that is, to use the pulse subtraction harmonic imaging mode with a mechanical index level from 0.22 to 0.25, which is a low level in accordance with our previous report [22]. Gain was adjusted to an optimal level, and the dynamic range was set at 45–50 dB.

The contrast agent Sonazoid (perflubutane microbubbles with a median diameter of 2–3 μm) was used at a dose of 0.0075 ml/kg administered by manual bolus injection, followed by 3.0 ml of normal saline (administered by H.I.). Contrast enhancement was observed during two phases: the vascular phase (from contrast agent injection to 1 min, which is the early phase) and late phase (15 min after injection), under breath-holding as often as possible. For all patients, the operator performing the US examinations was M.T. (who had 7 years of experience in US examination). All US images recorded digitally were reviewed using frame-by-frame playback at a later date by H.M. (who had 19 years of experience in US examination), and contrast enhancement in the inner and outer nodules of the HCC lesions was assessed in comparison with that in adjacent liver parenchyma as hyper-, iso-, or hypo-enhanced in appearance.

2.3. Contrast-enhanced CT

Contrast-enhanced CT with dynamic imaging was performed in all patients using the Lightspeed Ultra16 (GE Yokogawa Medical Systems, Hino, Japan) with injection of 100 ml of contrast medium (Iopamiron 350; Nihon Schering, Osaka, Japan) at 3 ml/s into the antecubital vein by means of a mechanical injection system (Mark V ProVis, MEDRAD, Warrendale, PA, USA). Imaging was performed with a 30-s delay between contrast medium administration and start of imaging for the hepatic artery-dominant phase, 80-s delay for the portal vein-dominant phase, and 180-s delay for the equilibrium phase. The contrast-enhanced CT findings were evaluated by M.Y., who had 28 years of experience in heaptology, and was blinded to the patient information.

2.4. Pathological examination of HCC lesions

Pathological examination was performed on specimens obtained from 9 HCC lesions by percutaneous US-guided needle biopsy using a Sonopsy C1 needle (Hakko, Tokyo, Japan). Separate sampling from the inner and outer nodules was performed for 2 HCC lesions, although only a single sample was taken from the other 7 HCC lesions due to technical difficulties. All needle biopsies were performed by S.O. after US examination, and the time lag between contrast-enhanced US examination and needle biopsy ranged from 1 to 14 days (mean 4.5 ± 4.1 days). Pathological results were obtained from the surgically resected specimen in the case of one HCC lesion, with the time lag between contrast-enhanced US examination and surgical treatment being 2 months.

2.5. Statistical analysis

All data were expressed as means ± SD or percentages. Statistical significance was analyzed by using the Chi-square test, and p-values <0.05 were considered to be significant. Statistical analysis was performed using the SPSS software package (Version 13.0J; SPSS Inc., Chicago, IL, USA).

3. Results

3.1. Non-contrast US findings in HCC

Grey-scale US showed 5 lesions with a hyperechoic outer nodule and hypoechoic inner nodule, 2 lesions with a hypoechoic outer nodule and isoechoic inner nodule, one lesion with an isoechoic outer nodule and hypoechoic inner nodule, and one lesion with a hypoechoic outer nodule and hyperechoic inner nodule. In these 9 lesions, grey-scale US could clearly discriminate the outer nodule from the inner nodule, and the diameter of the inner nodules ranged from 6.6 to 16.0 mm (mean 10.9 ± 2.9 mm). The remaining lesion

Table 1
Pathological results and contrast enhancement of hepatocellular carcinoma.

Case	Size (mm)	Pathology I/O	Inner nodule		Outer nodule	
			V	L	V	L
1	24	M/W[a]	Hyper	Hypo	Hypo	Iso
2	14.4	W	Hyper	Hypo	Hypo	Iso
3	23	W	Hyper	Iso	Hypo	Iso
4	39	M/W[b]	Hyper	Hypo	Hypo	Iso
5	25.1	W	Hyper	Hypo	Hypo	Iso
6	17.1	W	Hyper	Hypo	Hyper	Hypo
7	34.3	M	Hyper	Hypo	Iso	Iso
8	24.8	W	Hyper	Hypo	Hyper	Hypo
9	28.5	W	Hyper	Iso	Iso	Iso
10	31.1	M/W[a]	Hyper	Hypo	Hyper	Hypo

I/O: Inner nodule/outer nodule, V: vascular phase, L: late phase, W: well differentiated HCC, M: moderately differentiated HCC, Hyper: hyper-enhancement, Iso: iso-enhancement, Hypo: hypo-enhancement.
[a] Separate sampling for inner and outer nodules by needle biopsy.
[b] Assessment of pathological result on surgically resected specimen.

showed a hypoechoic appearance without any difference between the outer and inner nodules. Neither US nor contrast-enhanced CT detected ascites, vascular abnormality, portal vein thrombosis, or portal vein tumor thrombosis.

3.2. Contrast-enhanced US findings in HCC

Vascular-phase US images of the inner nodule were hyper-enhanced in appearance in all 10 lesions, and images of the outer nodule were hyper-enhanced in 3 lesions, iso-enhanced in 2, and hypo-enhanced in 5 (Table 1). As the contrast enhancement of the inner nodule was much stronger than that of the outer nodule in all lesions, dedifferentiation of the tumor was clearly demonstrated in this vascular phase. Late-phase images of the inner nodule showed a hypo-enhanced appearance in 8 lesions and iso-enhancement in 2. Meanwhile, late-phase images of the outer nodule were iso-enhanced in the 7 lesions that showed an iso- or hypo-enhanced appearance in the vascular phase, and hypo-enhanced in the 3 showing a hyper-enhanced appearance in the vascular phase (Tables 1 and 2 and Figs. 1 and 2). Neither the inner nodules nor the outer nodules had a hyper-enhanced appearance in the late phase. A late-phase hypo-enhanced appearance was significantly more frequent in the nodules showing early-phase hyper-enhancement (11/13) than in the nodules showing early-phase iso- or hypo-enhancement (0/7) in both the inner and outer nodules.

3.3. Pathological results and contrast enhancement in each nodule

Pathological examination of the 7 HCC lesions without separate nodule sampling revealed well-differentiated HCC in 6 lesions and moderately differentiated HCC in one. The remaining 3 lesions showed well-differentiated HCC in the outer nodule and moderately differentiated HCC in the inner nodule. Upon contrast-enhanced US, all inner nodules in the latter 3 lesions showed a hyper-enhanced appearance in the vascular phase and hypo-enhancement in the late phase. On the other hand, the outer nodule in 2 lesions showed a hypo-enhanced appearance in the vascular phase and iso-enhancement in the late phase, and that in one lesion showed a hyper-enhanced appearance in the vascular phase and hypo-enhancement in the late phase.

Table 2
Contrast enhancement in the outer and inner nodule.

	Vascular phase (Hyper/Iso/Hypo)	Late phase (Hyper/Iso/Hypo)
Outer nodule	3/2/5	0/7/3
Inner nodule	10/0/0	0/2/8

Hyper: Hyper-enhancement, Iso: iso-enhancement, Hypo: hypo-enhancement.

4. Discussion

The nodule-in-nodule appearance of HCC lesions, supported by radiological and pathological evidence, represents a characteristic feature of developing HCC [15–21]. Typical findings on contrast-enhanced CT/magnetic resonance imaging include a hypervascular spot within the iso- or hypo-vascular lesion. The outer nodule is generally considered to be at an earlier stage of carcinogenesis relative to the inner nodule in HCC, hence the nodule-in-nodule appearance.

A cardinal non-contrast US finding in HCC lesions with a nodule-in-nodule appearance is a hypoechoic nodule within a hyperechoic nodule, which was also the most common pattern in our study. However, as previously reported, focal hepatic lesions with nodule-in-nodule appearance show various patterns on the grey-scale sonogram, and one lesion in the current study appeared hypoechoic without showing any difference between the inner and outer nodules [23]. Therefore, hemodynamic-based imaging may be required to diagnose nodule-in-nodule-appearing tumors, and vascular-phase sonograms can be obtained easily with Sonazoid and have clearly demonstrated the difference in vascularity between the inner and outer nodules in HCC lesions, as in contrast-enhanced CT images. Similar to the results from previous studies using other kinds of microbubble contrast agents, the current study suggested that contrast-enhanced US with Sonazoid can offer at least the same rate of detecting characteristic HCC tumor vascularity as contrast-enhanced CT [24–26].

Late-phase appearance varied in the inner nodule, with 80% of nodules showing a hypo-enhanced appearance and 20% of nodules showing iso-enhancement. These results may be absolutely reasonable because late-phase wash-out following vascular-phase hyper-enhancement is considered to be typical findings in cases of HCC [11,12]. Meanwhile, outer nodules that were hypo- or iso-enhanced in the vascular phase showed an iso-enhanced appearance in the late phase, and those hyper-enhanced in the vascular phase showed hypo-enhancement in the late phase. As the inner nodule appears to be in the post-dedifferentiated state and thus in a more advanced stage of carcinogenesis relative to the outer nodule, it is logical to assume that, as HCC progresses, the inner nodule may eventually exhibit the same enhancement pattern seen later in the outer nodule. Thus, our results suggest that tumor neovascularity precedes the deficit in microbubble contrast accumulation during the dedifferentiation process of HCC. In fact, it is strongly speculated that developing HCC progresses from lesions with hypo- or iso-enhancement in the vascular phase and iso-enhancement in the late phase, to lesions with hyper-enhancement in the vascular phase and iso-enhancement in the late phase, and subsequently to lesions with hyper-enhancement in the vascular phase and hypo-enhancement in the late phase. Therefore, a late-phase observation alone may not always be sufficient in screening for HCC because it could fail to detect developing HCC with an iso-enhanced appearance in the late phase.

Phagocytosis of microbubbles by Kupffer cells is one of the theoretical mechanisms for the late-phase enhancement findings in contrast-enhanced US with Sonazoid [14]. Considering the relationship between Kupffer cell distribution and cellular differentiation in HCC, the microbubble-related enhancement patterns in the late phase in our study might be explained by this theory [5,6]. The Levovist contrast agent also accumulates in the liver, and it is

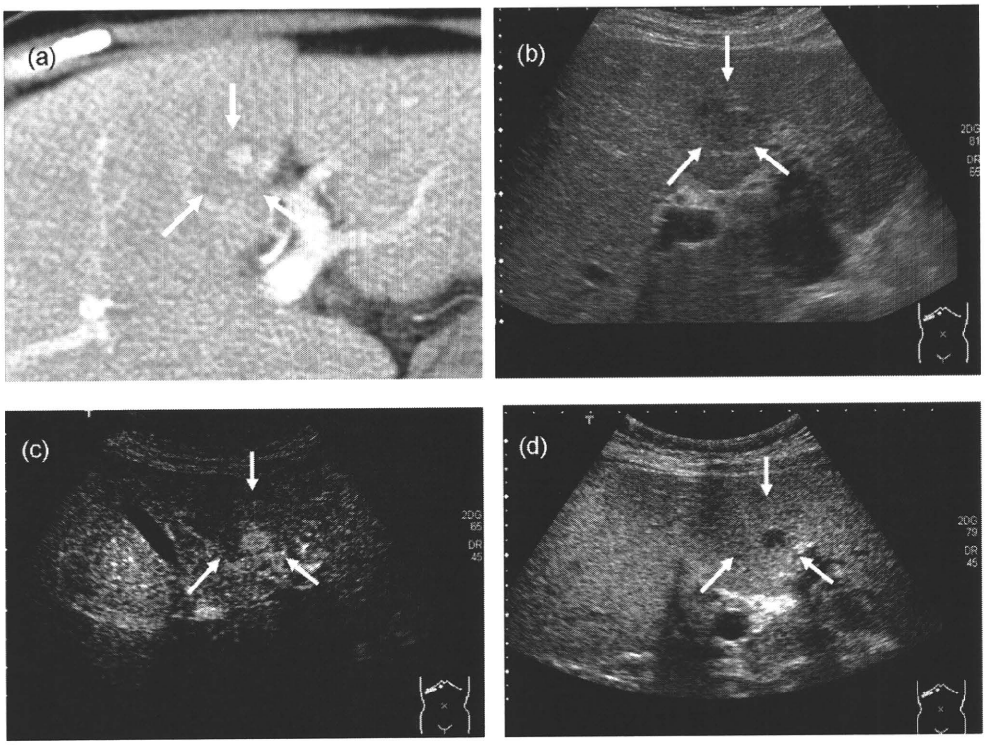

Fig. 1. A 69-year-old female, hepatitis C virus-related cirrhosis, HCC with nodule-in-nodule appearance (S4, 24 mm; case 1). (a) Contrast-enhanced CT, artery-dominant phase. HCC with hypovascular outer nodule and hypervascular inner nodule (arrows). (b) Grey-scale US. HCC with hypoechoic appearance (arrows). (c) Contrast-enhanced US, vascular phase. HCC with hypo-enhanced outer nodule and hyper-enhanced inner nodule (arrows). (d) Contrast-enhanced US, late phase. HCC with iso-enhanced outer nodule and hypo-enhanced inner nodule (arrows).

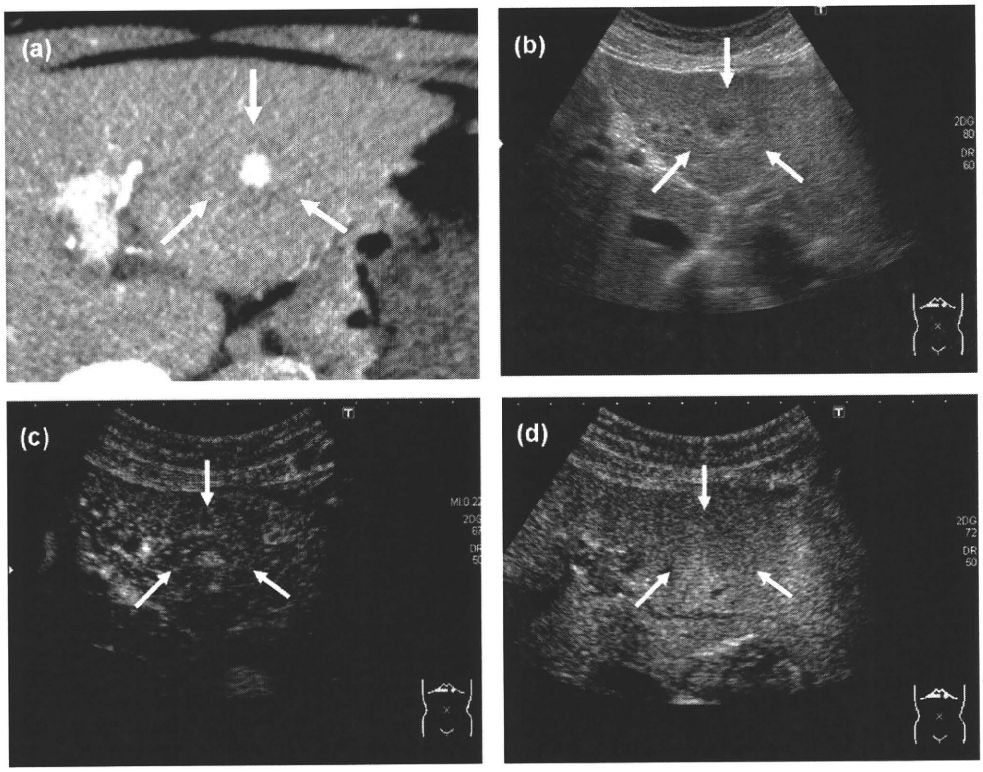

Fig. 2. A 74-year-old female, hepatitis C virus-related cirrhosis, HCC with nodule-in-nodule appearance (S3, 28.5 mm; case 9). (a) Contrast-enhanced CT, artery-dominant phase. HCC with isovascular outer nodule and hypervascular inner nodule (arrows). (b) Grey-scale US. HCC with hyperechoic outer nodule and hypoechoic inner nodule (arrows). (c) Contrast-enhanced US, vascular phase. HCC with iso-enhanced outer nodule and hyper-enhanced inner nodule (arrows). (d) Contrast-enhanced US, late phase. HCC with iso-enhanced outer and inner nodules (arrows).

reported that late-phase enhancement with this agent in well-differentiated HCC and benign regenerative nodules was similar to that in adjacent non-tumor liver parenchyma, whereas moderately differentiated HCC tended to have a washed-out appearance in this phase [11,12,27]. Meanwhile, in studies using the contrast agents SonoVue® (Bracco, Milan, Italy) and Definity® (Lantheus, North Billerica, MA, USA), which do not accumulate in the liver, hypo-enhancement or a washed-out appearance after the vascular-phase peak enhancement and an earlier wash-out were frequent and consistent with the degree of tumor differentiation in HCC [28,29]. These results with different contrast agents suggest that hypo-enhancement or wash-out findings may be common in spite of the type of US contrast agent used, and mechanisms other than Kupffer cell distribution might account for the late-phase enhancement pattern in HCC. However, as these possible explanations are still at a speculative level, further investigations are required to account for these findings.

Our study had several limitations. The first is that the histological results of all but one HCC were obtained from specimens obtained by percutaneous US-guided needle biopsy, and separate sampling from inner and outer nodules was performed in only 2 of the 9 HCC lesions biopsied. According to previous studies, the histological structure of the outer nodule in nodule-in-nodule-appearing lesions varies and can be diagnosed as: adenomatous hyperplasia, siderotic regenerative nodule, macroregenerative nodule, or well-differentiated HCC [15–19]. Assessment of the pathology of the surgically resected specimen might allow confirmation of agreement between the histological findings and the results of US with contrast enhancement. The second limitation is that our study consisted of a small number of subjects and lacked follow-up of the natural progression of HCC with nodule-in-nodule appearance. Further studies with large numbers of patients and with US follow-up of contrast-enhanced changes in each nodule during the period between diagnosis and treatment may be necessary to allow us to draw more definitive conclusions.

5. Conclusions

Dedifferentiation of HCC may be accompanied by changes in neovascularity prior to the reduction in microbubble contrast accumulation, with the latter possibly related to Kupffer cell distribution. Although late-phase ultrasonography with static microbubbles may have the advantage of easy and stable observation, vascular-phase contrast enhancement using Sonazoid dynamic microbubbles could allow early recognition of the dedifferentiation of HCC.

References

[1] Bosch FX, Ribes J, Borras J. Epidermiology of primary liver cancer. Semin Liver Dis 1999;19(3):271–85.
[2] Okuda K. Hepatocellular carcinoma. J Hepatol 2000;32(1 Suppl.):225–37.
[3] Tong MJ, Blatt LM, Kao VW. Surveillance for hepatocellular carcinoma in patients with chronic viral hepatitis in the United States of America. J Gastroenterol Hepatol 2001;16(7):553–9.
[4] Larcos G, Sorokopud H, Berry G, Farrell GC. Sonographic screening for hepatocellular carcinoma in patients with chronic hepatitis or cirrhosis: an evaluation. AJR Am J Roentgenol 1998;171(2):433–5.
[5] Tanaka M, Nakashima O, Wada Y, Kage M, Kojiro M. Pathomorphological study of Kuppfer cells in hepatocellular carcinoma and hyperplastic nodular lesions in the liver. Hepatology 1996;24(4):807–12.
[6] Imai Y, Murakami T, Yoshida S, et al. Super paramagnetic iron oxide enhanced magnetic resonance images of hepatocellular carcinoma: correlation with histological grading. Hepatology 2000;32(2):205–12.
[7] Hayashi M, Matsui O, Ueda K, et al. Correlation between the blood supply and grade of malignancy of hepatocellular nodules associated with liver cirrhosis: evaluation by CT during intraarterial injection of contrast medium. Am J Roentgenol 1999;172(4):969–76.
[8] Kremkau FW. Diagnostic ultrasound: principles and instruments. 4th ed. Philadelphia: WB Saunders; 1993.
[9] Mitchell DG. Color Doppler imaging: principles, limitations, and artifacts. Radiology 1990;177(1):1–10.
[10] Goldberg BB. Ultrasound contrast agents. Martin Dunitz Ltd.; 1997.
[11] Rettenbacher T. Focal liver lesions: role of contrast-enhanced ultrasound. Eur J Radiol 2007;64(2):173–82.
[12] Quaia E. Microbubble ultrasound contrast agents: an update. Eur Radiol 2007;17(8):1995–2008.
[13] Marelli C. Preliminary experience with NC100100, a new ultrasound contrast agent for intravenous injection. Eur Radiol 1999;9(Suppl. 3):S343–6.
[14] Watanabe R, Matsumura M, Munemasa T, Fujimaki M, Suematsu M. Mechanism of hepatic parenchyma-specific contrast of microbubble-based contrast agent for ultrasonography: microscopic studies in rat liver. Invest Radiol 2007;42(9):643–51.
[15] Matsui O, Kadoya M, Kameyama T, et al. Adenomatous hyperplastic nodules in the cirrhotic liver: differentiation from hepatocellular carcinoma with MR imaging. Radiology 1989;173(1):123–6.
[16] Mitchell DG, Rubin R, Siegelman ES, Burk Jr DL, Rifkin MD. Hepatocellular carcinoma within siderotic regenerative nodules: appearance as a nodule within a nodule on MR images. Radiology 1991;178(1):101–3.
[17] Muramatsu Y, Nawano S, Takayasu K, et al. Early hepatocellular carcinoma: MR imaging. Radiology 1991;181(1):209–13.
[18] Winter 3rd TC, Takayasu K, Muramatsu Y, et al. Early advanced hepatocellular carcinoma: evaluation of CT and MR appearance with pathologic correlation. Radiology 1994;192(2):379–87.
[19] Sadek AG, Mitchell DG, Siegelman ES, Outwater EK, Matteucci T, Hann HW. Early Hepatocellular carcinoma that develops within macroregenerative nodules: growth rate depicted at serial MR imaging. Radiology 1995;195(3):753–6.
[20] Kojiro M. 'Nodule-in-nodule' appearance in hepatocellular carcinoma: its significance as a morphologic marker of dedifferentiation. Intervirology 2004;47(3–5):179–83.
[21] Zheng RQ, Zhou P, Kudo M. Hepatocellular carcinoma with nodule-in-nodule appearance: demonstration by contrast-enhanced coded phase inversion harmonic imaging. Intervirology 2004;47(3–5):184–90.
[22] Maruyama H, Takahashi M, Ishibashi H, et al. Ultrasound-guided treatments under low acoustic power contrast harmonic imaging for hepatocellular carcinomas undetected by B-mode ultrasonography. Liver Int 2009;29(5):708–14.
[23] Ishida Y, Nagamatsu H, Koga H, Yoshida H, Kojiro M, Sata M. Hepatocellular carcinoma with a "nodule-in-nodule" appearance reflecting an unusual dilated pseudoglandular structure. Int Med 2008;47(13):1215–8.
[24] Numata K, Tanaka K, Kiba T, et al. Contrast-enhanced, wide-band harmonic gray scale imaging of hepatocellular carcinoma. Correlation with helical computed tomographic findings. J Ultrasound Med 2001;20(2):89–98.
[25] Giorgio A, Ferraioli G, Tarantino L, et al. Contrast-enhanced sonographic appearance of hepatocellular carcinoma in patients with cirrhosis: comparison with contrast-enhanced helical CT appearance. AJR Am J Roentgenol 2004;183(5):1319–26.
[26] Bolondi L, Gaiani S, Celli N, et al. Characterization of small nodules in cirrhosis by assessment of vascularity: the problem of hypovascular hepatocellular carcinoma. Hepatology 2005;42(1):27–34.
[27] Yoshizumi H, Maruyama H, Okugawa H, et al. How to characterize non-hypervascular hepatic nodules on contrast-enhanced computed tomography in chronic liver disease: feasibility of contrast-enhanced ultrasound with a microbubble contrast agent. J Gastroenterol Hepatol 2008;23(10):1528–34.
[28] Nicolau C, Catalá V, Vilana R, et al. Evaluation of hepatocellular carcinoma using SonoVue, a second generation ultrasound contrast agent: correlation with cellular differentiation. Eur Radiol 2004;14(6):1092–9.
[29] Jang HJ, Kim TK, Burns PN, Wilson SR. Enhancement pattern of hepatocellular carcinoma at contrast-enhanced US: comparison with histologic differentiation. Radiology 2007;244(3):898–906.